CHALMERS
UNIVERSITY OF TECHNOLOGY

The Implication of Emission Control Systems on the Mass and Energy Balances of the Kraft Pulp Mill Process

A Case Study of Södra Cell Mönsterås's Recovery Boiler

Master's thesis in Innovative and Sustainable Chemical Engineering

JESPER JOHANSSON
SAMUEL OLSSON

DEPARTMENT OF SPACE, EARTH AND ENVIRONMENT
CHALMERS UNIVERSITY OF TECHNOLOGY
Gothenburg, Sweden 2024
www.chalmers.se

MASTER'S THESIS SEEX30 2024

The Implication of Emission Control Systems on the Mass and Energy Balances of the Kraft Pulp Mill Process

A Case Study of Södra Cell Mönsterås's Recovery Boiler

JESPER JOHANSSON
SAMUEL OLSSON

CHALMERS
UNIVERSITY OF TECHNOLOGY

Department of Space, Earth and Environment
Chalmers University of Technology
Gothenburg, Sweden 2024

The Implication of Emission Control Systems on the Mass and Energy Balances of the Kraft Pulp Mill Process

A Case Study of Södra Cell Mönsterås's Recovery Boiler

JESPER JOHANSSON & SAMUEL OLSSON

Supervisors:
Jenny Larfeldt, Södra
Jakob Johansson, Space, Earth and Environment
Rosa Citra Aprilia, Space, Earth and Environment

Examiner:
Fredrik Normann, Space, Earth and Environment

Master's thesis 2024
Department of Space, Earth and Environment
Division of Energy Technology
Chalmers University of Technology
SE-412 96 Gothenburg
Sweden
Telephone +46 31 772 1000

Cover: Södra Cell Mönsterås's kraft pulp mill

Typeset in LaTeX
Gothenburg, Sweden 2024

The Implication of Emission Control Systems on the Mass and Energy Balances of the Kraft Pulp Mill Process
A Case Study of Södra Cell Mönsterås's Recovery Boiler
Jesper Johansson & Samuel Olsson
Department of Space, Earth and Environment
Division of Energy Technology
Chalmers University of Technology

Abstract

This master's thesis concludes on the mass and energy balances of the kraft pulp mill process and investigates the possible implications in connection to new emission control systems. The work is based on a case study of the recovery boiler at Södra Cell in Mönsterås. Key aspects include the energy and element balances occurring in the boiler and the emission of NO_x and SO_x. Three primary emission control measures are evaluated: injection of ammonia solutions (SNCR), injection of ammonia-containing gas (dissolver off gas), and the injection of scrubber effluent.

The process model is based on previous work and validated by comprehensive data collection from the reference plant. The model is implemented in the software Aspen Plus. The model is zero-dimensional and equilibrium-based and cannot describe the effects of spatial distribution of air and temperature within the boiler or processes controlled by kinetic-based reactions.

The result shows that the implementation of water-diluted ammonia injection with the potential to reduce NO_x emissions by 45 % does not significantly affect flue gas temperature. While the use of dissolver off gas is advantageous, due to the utilisation of a waste stream, current ammonia levels from the dissolver off gas is insufficient for achieving significant SNCR effects compared to water-diluted ammonia injection, with a difference of 0.69 mol NH_3/s. Recycling scrubber effluent does not significantly alter the sulphidity of the flue gas but does increase reduction efficiency of the smelt, thereby reducing the need for make-up chemicals.

The derived model is useful for describing the overall implications of the recovery boiler's mass and energy balances and could be used to quantify the effects of other process modifications. The work should be complemented with more detailed design tools.

Keywords: Södra Mönsterås, kraft pulp mill, recovery boiler, Aspen Plus, emission control, primary measures, NO_x, SOx

Effekterna av Utsläppskontrollsystem på Mass- och Energibalanserna i Kraftmassabruksprocessen
En Fallstudie av Södra Cell Mönsterås Sodapanna
Jesper Johansson & Samuel Olsson
Institutionen för rymd-, geo- och miljövetenskap
Avdelningen för Energiteknik
Chalmers Tekniska Högskola

Sammanfattning

Detta examensarbete sammanfattar mass- och energibalanserna för kraftmassabruksprocessen och undersöker de möjliga effekterna i samband med nya utsläppskontrollsystem. Arbetet är baserat på en fallstudie av sodapannan vid Södra Cell i Mönsterås. Viktiga aspekter är energi- och elementbalanserna i pannan samt utsläppen av NO_x och SO_x. Tre primära åtgärder för utsläppskontroll utvärderas: injektion av vattenlöst ammoniak (SNCR), injektion av ammoniakhaltig gas (imånga) och injektion av skrubbervätska.

Processmodellen är baserad på tidigare arbete och validerad genom omfattande datainsamling från referensanläggningen. Modellen är implementerad i programvaran Aspen Plus. Modellen är nolldimensionell och jämviktsbaserad och kan därmed inte beskriva effekterna av rumslig fördelning av luft och temperatur i pannan eller processer som styrs av kinetikbaserade reaktioner.

Resultatet visar att implementeringen av vattenlöst ammoniakinjektion med potential att minska NO_x-utsläppen med 45 % inte påverkar rökgastemperaturen nämnvärt. Även om användningen av imångan är fördelaktig, på grund av användningen av en avfallsström, är de nuvarande ammoniaknivåerna från imångan otillräckliga för att uppnå betydande SNCR-effekter jämfört med vattenlöst ammoniakinjektion, med en skillnad på 0.69 mol NH_3/s. Återvinning av skrubbervätskan förändrar inte rökgasens sulfiditet nämnvärt i pannan, men ökar reduktionsgraden i smältan och minskar därmed behovet av tillsatskemikalier.

Den framtagna modellen är användbar för att beskriva de övergripande effekterna av sodapannans mass- och energibalanser och kan användas för att kvantifiera effekterna av andra processmodifieringar. Arbetet bör kompletteras med mer detaljerade designverktyg.

Nyckelord: Södra Mönsterås, kraftmassabruk, sodapanna, Aspen Plus, utsläppskontroll, primära åtgärder, NO_x, SO_x

Acknowledgements

We extend our gratitude to all those who have supported and contributed to this thesis.

A special thank you goes to our examiner, Fredrik Normann, and our supervisor, Jakob Johannson, for their valuable input and thorough assistance throughout this work. We have appreciated our regular meetings that steered us in the right direction as well as engaging discussions. We would also like to thank Rosa Citra Aprilia who supported us in the initial stages of our work and provided valuable information.

A heartfelt thank you to Jenny Larfeldt, our supervisor at Södra, whose exceptional guidance and support made this project possible. From providing crucial data to arranging meetings and even booking hotel rooms, your assistance have been very helpful along the way.

Additionally, we give our gratitude to Södra as a whole for facilitating our visit to Mönsterås for an entire week. Thanks to Francis Gillet, Mats Häll, and Magnus Tyrberg for extending a warm welcome in Mönsterås and providing us with various data during the project.

Finally, a last thank you to Samuel Myrberg for an enjoyable collaborative workflow between our parallel projects and interesting discussions throughout the thesis.

Jesper Johansson & Samuel Olsson, Gothenburg, May 2024

Contents

List of Figures

List of Tables

1

Introduction

In response to the escalating environmental concerns, industries around the world are constantly improving their operations and developing new strategies to reduce the emissions of greenhouse gases. Some of the most concerning pollutants from the pulp and paper industries are nitrogen oxides, NO_x, and sulphur oxides, SO_x, which are formed from combustion at high temperatures. Exposure to both nitrogen and sulphur oxides result in direct negative health effects on living organisms and they contribute to the acidification of forests, soil, and waters. NO_x also contributes to acidic rain as well as eutrophication when dissolved in water. Considering a conventional kraft paper pulp mill, utilisation of the recovery boiler and lime kiln are the main sources of such emissions as a result of combustion at high temperatures [1]. There have been many improvements regarding the NO_x and SO_x reduction for industries throughout the years, but there is still a lot of potential to implement technology for emission control measures to meet the future emission regulations.

As part of these control measures, emission reduction commitments for the period 2020-2029 and 2030 and forward have been implemented, increasing the regulations on emissions of NO_x and SO_x within the EU member states. In Sweden, the emission reduction commitments for the period 2020-2029 have been achieved for both NO_x and SO_x, as well as the commitment for SO_x from 2030 and beyond. However, to comply with the commitments for NO_x from 2030 and beyond, a further reduction of 40 % compared to the emissions in 2021 is needed cumulatively across all relevant sectors [2].

Incentives such as NO_x fees have also been enforced in different energy sectors as a result of the increasing regulations. In Sweden, the fee is 50 SEK per kg of emitted NO_x annually, and the fee is repaid based on how much energy each industry produces. This emission penalty is not applied for boilers in the pulp industry today, but new regulations suggest that the energy credited from recovery boilers should be re-formulated from 100 % to 60 % until 2030 and thereby put a price on emitting NO_x [3].

There are requirements for the Best Available Technologies (BAT) covered by EU's Industrial Emissions Directive (IED). The directive sets requirements for emissions to air from kraft recovery boilers that must be within specific emission ranges annually [4]. Presently, many paper pulp mills manage to fulfill the requirements for BAT. However, anticipating future regulations proposed by the EU, concerns regarding the emission commitments have emerged, resulting in increased interest in emission control. One company that has opted to address these growing concerns is Södra Cell in Mönsterås.

Therefore, a case study will be conducted at Södra Cell Mönsterås to investigate possibilities for implementing technologies for emission control in their kraft recovery boiler.

1.1 Aim

The aim of this project is to quantify the impact of implementing new emission control technologies on the mass and energy balances of a kraft recovery boiler. The project will also construct the heat and mass balance process model and validate it against industrial data and a literature review.

The process model is constructed in the software Aspen Plus based on industrial data from Södra's pulp mill in Mönsterås, Sweden. The emission control technologies evaluated include water-diluted ammonia injection, dissolver off gas injection, and recycling of scrubber effluent. The results from the model include the impact on the high-temperature chemistry occurring in the recovery boiler, correlations between key performance indicators, process changes, and the formation of NO_x and SO_x.

2

Theory

In this chapter, a general explanation of the kraft recovery process is provided, as well as a more in-depth description of the recovery boiler, including descriptions of the chemical processes taking place in the different parts of the unit. The general formation routes for NO_x and SO_x, along with the sodium and sulphur balance in the recovery boiler are also presented in this chapter, followed by the currently available technology for emission reduction.

2.1 The kraft pulp mill and chemical recovery process

The kraft process performed at Södra involves transforming wood into wood pulp. Wood pulp consists mainly of cellulose fibers and is one of the main components in paper production. The process is known for its ability to decompose the wood chips into pulp using a mix of white liquor and steam. White liquor is a solution that consists of sodium hydroxide (NaOH) and sodium sulphide (Na_2S) [5].

The process include several steps, preparation of wood chips, cooking, washing, bleaching, and drying. The wood chip preparation is the start of the process where the timber, softwood or hardwood, is debarked and chipped into small pieces. The cooking stage takes place in the pulp digester, where white liquor and steam are added. The purpose is to break the bonds between lignin, hemicellulose, and cellulose in the wood and remove the lignin by dissolution. After cooking, the pulp is washed to remove the spent cooking chemicals and lignin. The washing plant also addresses chemical recovery, chemical demand in subsequent bleaching steps, as well as obtaining a clean product. The product is then bleached to further remove color and improve brightness. Various chemicals like chlorine, chlorine dioxide, hydrogen peroxide, or oxygen can be used in this step. When the desired result is obtained the pulp needs to be dried to attain the right moisture content. The final wood pulp product can then be used to manufacture paper and other cellulose-based products [5].

Furthermore, one of the key features of the kraft process is the high chemical recovery efficiency. Figure 2.1 illustrates a simplified flowsheet of the kraft recovery process that includes the cooking chemical cycle and the lime cycle. This stage of the process enables the recycling of pulping chemicals (NaOH and Na_2S), which minimise chemical consumption, and also creates energy generation due to the combustion of black liquor in the recovery boiler [6].

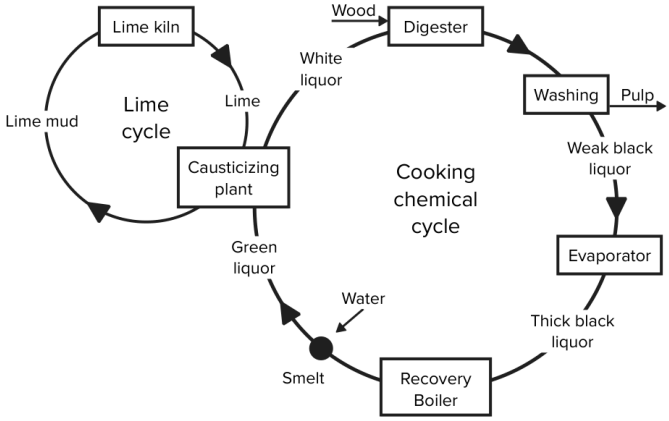

Figure 2.1: The kraft recovery process.

Figure 2.1 shows that during cooking in the digester, black liquor is formed, which contains dissolved lignin, spent cooking chemicals, and other by-products. When washing the pulp the weak black liquor is separated from the pulp and enters the multi-effect evaporators to remove water content and obtain thick black liquor. The recovery boiler burns the black liquor which generates heat and releases sodium compounds consisting mainly of sodium carbonate (Na_2CO_3) and sodium sulphide (Na_2S) which form the so-called char bed or molten smelt. The smelt is then extracted from the recovery boiler and enters a smelt dissolver tank where the sodium compounds are dissolved in water to form green liquor [7]. The green liquor then enters the causticizing plant. Here, the burned lime (CaO) from the lime kiln reacts with water to form $Ca(OH)_2$, also known as 'slaked lime'. The calcium hydroxide is then mixed with the green liquor (Na_2CO_3) in causticization vessels and the reaction forms NaOH and $CaCO_3$ as can be seen in Equation (2.1) [8].

$$Na_2CO_3 + CaO + H_2O \rightarrow 2\,NaOH + CaCO_3 \tag{2.1}$$

Calcium carbonate is separated from the white liquor and rewashed before being fed back into the lime kiln for reburning, closing the lime cycle. Na_2S as being part of the green liquor goes through the whole causticizing process and ends up in the white liquor together with the sodium hydroxide. The white liquor is then recovered to the digester [8].

As mentioned, the recycled lime ($CaCO_3$) from the white liquor preparation enters the rotary lime kiln together with makeup (added to compensate for chemical losses) lime mud. The lime sludge is then heated to a high temperature and reburnt into calcium oxide which can be fed back to the causticizing plant. The reaction that takes place in the lime kiln can be seen in Equation (2.2).

$$CaCO_3 \rightarrow CaO + CO_2 \tag{2.2}$$

The causticization process requires approximately 250 kg of calcium oxide per tonne of pulp produced. Therefore, the lime cycle is a very important part of the pulp mill process and is essential to avoid the expensive costs of make-up lime [8].

2.2 The recovery boiler

The purpose of the recovery boiler is to use thick black liquor as a source of fuel to produce superheated steam in the top region and to create smelt in the lower region. The heat released from the combustion of the organic matter of the lignin can be generated as superheated steam with the help of superheaters, boiler banks, and economisers. The superheated steam can further be used to power various processes in the mill, generating electricity through a turbine that produces low-pressure steam for district heating. The thick black liquor, with a dry solid content of 65-85 %, is obtained from the evaporation steps and then sprayed into the lower part of the recovery boiler. The molten smelt, containing mainly Na_2CO_3, Na_2S, and Na_2SO_4 is formed due to combustion in flight when the black liquor is burned in an oxygen-deficient environment [7].

The air supply to the recovery boiler is regulated at different sections of the furnace through primary, secondary, and tertiary air nozzles, as shown in Figure 2.2. In newer boilers, a quaternary air nozzle is common. Each injection serves a different purpose in the boiler due to the intricate chemical process that takes place. Both the efficiency of the reduction and the steam production are greatly affected by the arrangement of the air injection [9].

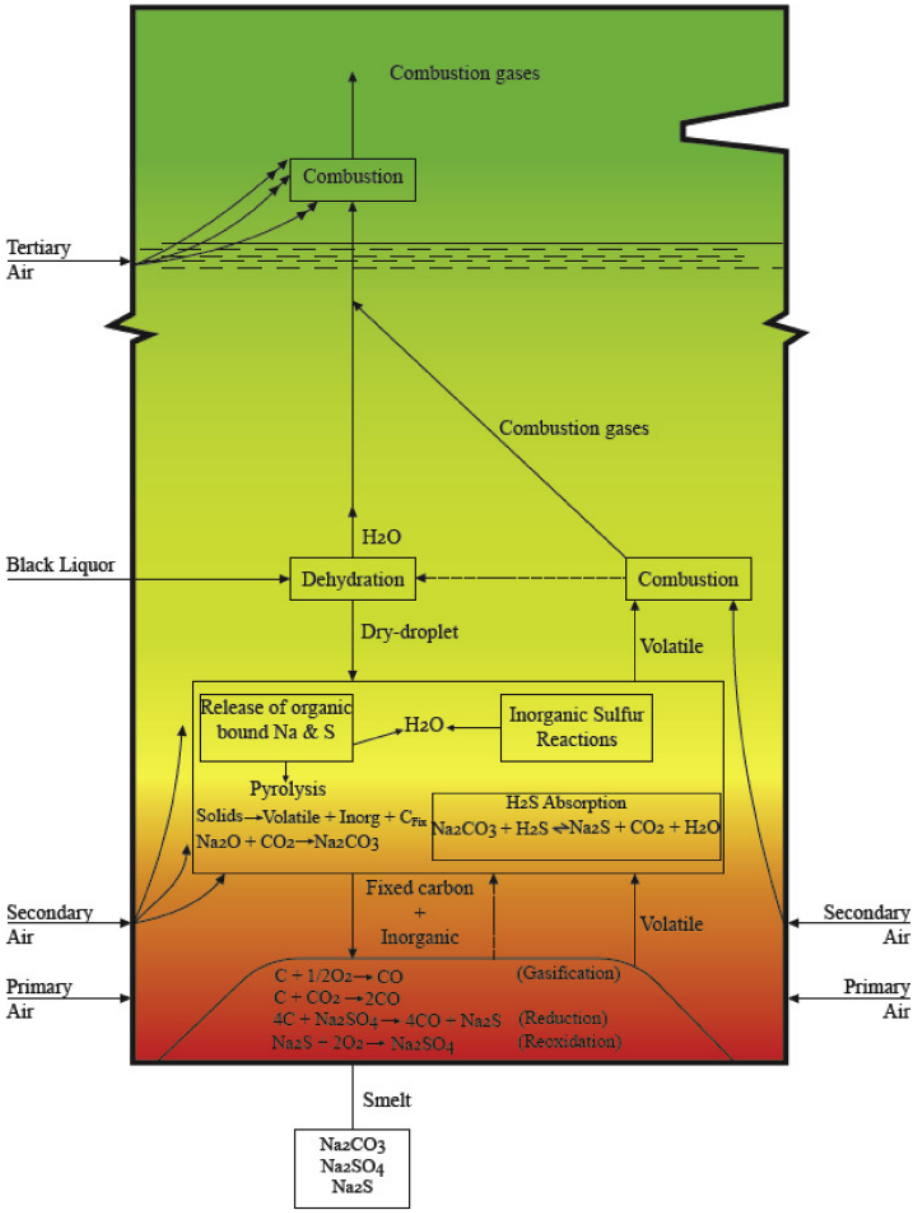

Figure 2.2: The main reactions in a recovery boiler at a kraft process [9].

The recovery boiler is a very complex furnace with several different physio-chemical reactions happening almost simultaneously, both exothermic and endothermic. To simplify the recovery boiler, it is divided into five different sections: steam production, combustion, drying, pyrolysis, and gasification followed by reduction. Figure 2.2 provides an overview of the main events and reactions occurring within the recovery boiler. Initially, black liquor droplets are sprayed into the boiler, where they are exposed to exhaust gases from the bottom of the boiler, leading to the evaporation of the remaining moisture.

Subsequently, the dry black liquor droplets continue downward and mix with secondary air and volatiles from the reduction stage, initiating pyrolysis. During this phase, organic-bound sodium and sulphur are released from the droplets and react with water, while inorganic sulphur also undergoes reactions with water. The solids

break down to form a mixture of gaseous byproducts such as CO_2, CO, SO_2, CH_4, H_2O, total reduced sulphur (TRS) volatiles (CH_3SH, CH_3SCH_3, $CH_3S_2CH_3$, H_2S), and a porous particulate material [9]. The key reactions occurring in the pyrolysis are outlined below:

$$\text{Solids} \rightarrow \text{Volatiles} + \text{Inorganic material} + \text{Fixed carbon} \tag{2.3}$$

$$Na_2O + CO_2 \rightarrow Na_2CO_3 \tag{2.4}$$

Simultaneously, H_2S will react with the Na_2CO_3 to form:

$$Na_2CO_3 + H_2S \rightarrow Na_2S + CO_2 + H_2O \tag{2.5}$$

Afterward, the porous particulate material, consisting mainly of Na_2CO_3, Na_2S, Na_2SO_4, and fixed carbon, reacts with the primary air in the bottom region of the boiler. The main reactions can be seen below.

$$C + \frac{1}{2}O_2 \rightarrow CO \tag{2.6}$$

$$C + H_2O \rightarrow CO + H_2 \tag{2.7}$$

$$C + CO_2 \rightarrow 2CO \tag{2.8}$$

$$CO + \frac{1}{2}O_2 \rightarrow CO_2 \tag{2.9}$$

The combustion that occurs in the reactions above, from the fixed carbon and the O_2 from the primary air, is exothermic and provides the energy required for the endothermic reactions in the reduction zone. The aim here is to use the remaining carbon to react with Na_2SO_4 yielding Na_2S. Although additional reactions also take place, but to a lesser degree, as shown below.

$$4C + Na_2SO_4 \rightarrow 4CO + Na_2S \tag{2.10}$$

$$2C + Na_2CO_3 \rightarrow 3CO + 2Na \tag{2.11}$$

$$Na_2S + 2O_2 \rightarrow Na_2SO_4 \tag{2.12}$$

Since Na_2S is the desired product, it is important to prevent its reoxidation back to Na_2SO_4 in order to obtain a high reduction efficiency. Therefore, to prevent the reaction in Equation 2.12, it is essential to maintain an oxygen-deficient environment. The smelt will then consist of a molten salt mixture, mainly composed of Na_2CO_3 and Na_2S. The reduction efficiency (RE) is calculated using the following equation:

$$\mathrm{RE}(\%) = \frac{\mathrm{Na_2S}\ (mol\%)}{\mathrm{Na_2S}\ (mol\%) + \mathrm{Na_2SO_4}\ (mol\%)} \tag{2.13}$$

Moreover, higher concentrations of potassium in the black liquor favor the formation of potassium salts in the smelt, such as K_2CO_3. Usually, potassium content in the black liquor is significantly lower compared to sodium, thus leading to lower amounts of potassium compounds in the smelt. Potassium behaves similarly as sodium in the recovery boiler due to their equal number of valence electrons, and potassium is, therefore, referred to as a sodium equivalent. The molar mass ratio between the two is 0.59 kg Na per kg K [10].

The gases formed during the pyrolysis stage, as well as the volatiles from the lower region will at the same time combust with the O_2 from the secondary and tertiary air to produce energy for the steam generation [10]. Carbon monoxide (CO) is another emission produced during combustion processes. It is typically oxidised to CO_2, but a small fraction exits as CO in the flue gas. This can result from poor combustion conditions, such as inadequate burning and mixing. Notably, elevated CO values often correlate with reduced oxygen availability during combustion, since this can minimise NO_x emissions [4].

The tertiary air is also used for further combustion in order to reduce overall emissions, the most common being NO_x, CO, and TRS. A quaternary air nozzle could further help reduce unwanted pollutants. In addition, different operating conditions and purification methods will also affect the result. The flue gas leaving the recovery boiler mainly consists of N_2, CO, CO_2, H_2O, and H_2. Besides these main components, it may contain other species such as NO_x, SO_x, TRS, Na_2SO_4, HCl, and CH_3SH [10].

A smaller fraction of the sodium and potassium salts that are formed in the lower part of the furnace ends up in the flue gas through dust formation, where potassium compounds are more volatile than sodium compounds due to its lower molar mass. Chlorine enriched in black liquor also contributes to the particulate formation of NaCl and KCl, along with gaseous HCl [10]. The chemical interaction between these species will be explained in Section 2.2.2.

2.2.1 Sulphidity, sodium and sulphur chemistry

The term 'sulphidity' in the kraft process can have different meanings depending on the stage of the process being considered. When considering the sulphidity of the entire kraft or 'sulphate' pulping process, it can be defined as the percentage molar ratio of Na_2S to the active alkali (AA), effective alkali (EA), or titratable alkali (TTA), as shown in the equations below:

$$\mathrm{AA} = \mathrm{NaOH} + \mathrm{Na_2S} \tag{2.14}$$

$$\mathrm{EA} = \mathrm{NaOH} + \frac{1}{2}\,\mathrm{Na_2S} \tag{2.15}$$

$$\mathrm{TTA} = \mathrm{NaOH} + \mathrm{Na_2S} + \mathrm{Na_2CO_3} \tag{2.16}$$

The sulphidity equation most commonly used is the one with respect to the active alkali (AA), as shown below:

$$\text{sulphidity}(\%) = \frac{\text{Na}_2\text{S}\ (mol\%)}{\text{NaOH}\ (mol\%) + \text{Na}_2\text{S}\ (mol\%)} \cdot 100 \tag{2.17}$$

The digester design establishes target values for sulphidity, AA, and TTA to get a desirable product. The sulphidity levels can differ depending on the type of timber used. Hardwood has a lower sulphidity compared to softwood pulping which can affect the quality of the product. Sulphidity does not contribute to increased pulp yield. However, the presence of hydrogen sulphide (HS^-) ions significantly enhances selectivity and delignification rate during kraft pulping without directly protecting the cellulosic material. In addition, due to its significant impact on delignification rate, HS^- ions result in shorter cooking times to achieve the wanted kappa number (an indicator of residual lignin content in the pulp). This shortened cooking time reduces exposure to alkali and/or cooking temperatures, ultimately increasing pulp yield. Additionally, the reduced fiber degradation can be interpreted as improved pulp strength [11].

The sulphidity for the black liquor entering the boiler can be described by the variations in total molar content of sulphur and sodium in the liquor, expressed as the S/Na_2 ratio. The same expression can also be used to describe the molar sulphur-to-sodium ratio in the flue gas, which will be further explained in Section 2.2.2. High sulphidity, along with the presence of oxidised sulphur-sodium salts such as Na_2SO_4 and Na_2SO_3 in the recovery cycle, contribute to an increase in the S/Na_2 ratio for the black liquor. In general, the sulphidity levels and S/Na_2 ratios of black liquors are often higher in Scandinavian pulp mills compared to North America. The S/Na_2 ratio usually lies between 0.35 to 0.5 in Scandinavia while it ranges between 0.2 to 0.3 in North America [10].

The ideal case would be if all the various sulphur and sodium compounds were converted to Na_2S and Na_2CO_3 in the smelt. However, in practice, the process is more intricate. Figure 2.3 shows a simplified illustration of the sulphur and sodium balance in a typical recovery boiler [10].

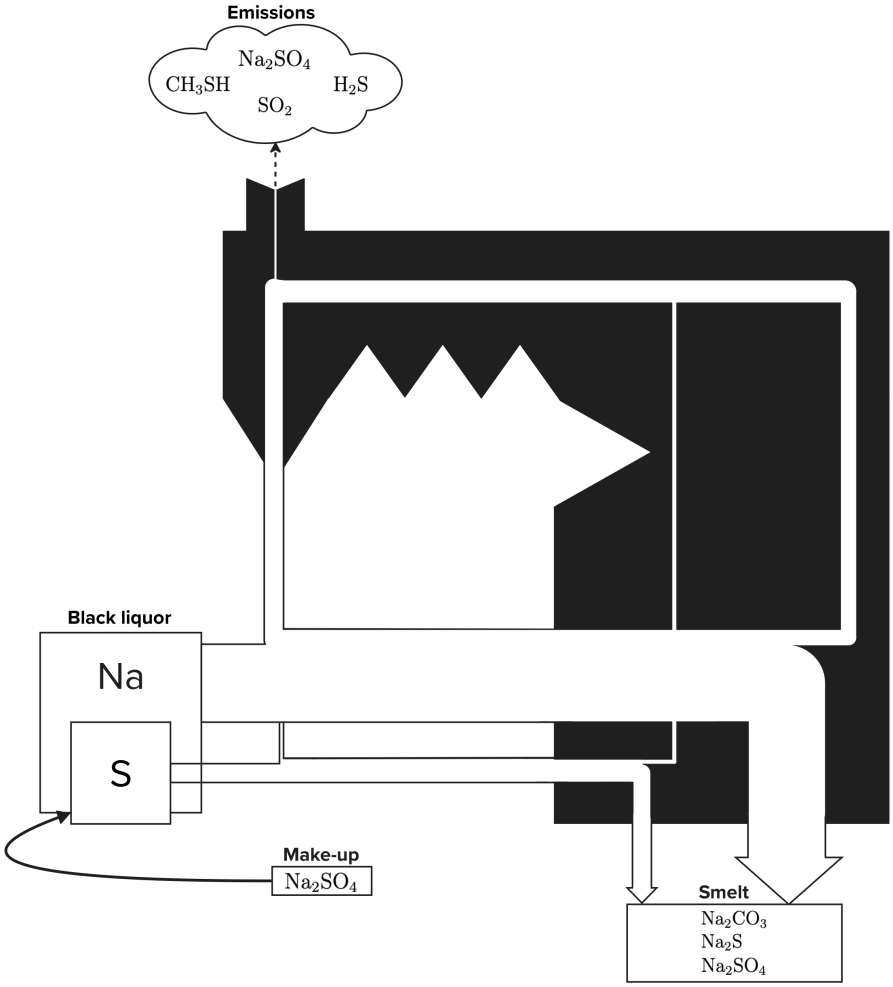

Figure 2.3: Sulphur and sodium balance in a typical recovery boiler.

The composition of sodium and sulphur in black liquor can differ significantly across various processes, or even for the same boiler, and this variation affects the sulphur and sodium balances. Figure 2.3 represents an approximate amount of the sulphur and sodium entering the boiler, as well as the balances occurring inside. Initially, the sulphur and sodium from black liquor enter the recovery boiler, and instead of just reacting to form Na_2CO_3 and Na_2S as the ideal case, they are also transformed into Na_2SO_4 in the smelt [10].

A significant portion of both sulphur and sodium is transported by the combustion gases upwards in the boiler, primarily as Na_2SO_4 dust and sulphur-containing gases. The majority of sodium and sulphur dust is captured and removed from the flue gases through an electrostatic precipitator (ESP). The captured dust is then blended with the fresh black liquor and reintroduced into the boiler. Finally, a minor fraction of the sodium and sulphur exits the process as emissions in the flue gases. The primary emission consists of Na_2SO_4, SO_2, H_2S and CH_3SH. Additionally, a make-up stream of Na_2SO_4 is introduced into the black liquor [10].

The vaporisation of sulphur and sodium from the bed depends heavily on the temperature in the furnace. For decreased bed temperatures, the release of gaseous sulphur increases linearly while gaseous sodium decreases at a much higher rate. Maintaining a bed temperature of approximately 1000 °C minimises the release for both gaseous sulphur and sodium [10].

2.2.2 Sulphur oxides and hydrogen chlorine formation routes

The formation of sulphur oxides, SO_x, mainly stems from the oxidation of fuel-bound sulphur, with the most prevalent species being SO_2 [12]. Other sulphur-related emissions include emissions of TRS, which result from incomplete combustion. In the presence of oxygen, TRS is oxidised to SO_2 [4].

The formation of the sulphur gases, SO_2 and TRS, begins when sulphur enters the recovery boiler through the black liquor in which it mainly exists as inorganic sulphur compounds, with the dominating forms being sulphide and sulphate. About 30-40 % of the sulphur present in black liquor exists as organic sulphur compounds [13]. The sulphate that ends up in the bed of the furnace is reduced by reducing gases (H_2 or CO) or char in the bed to Na_2S. The sulphate can also be vaporised in the form of H_2S or COS and is carried away by the flue gas. In the lower furnace in which there are reducing conditions, sulphur gases exist mainly as H_2S and as it moves toward the upper part of the furnace where there are oxidising conditions it reacts with oxygen to form SO_2 [10].

The sulphidity in the flue gas has a major impact on the formation of SO_2, and the chemistry in the flue gas and dust is almost entirely controlled by this S/Na_2 ratio. Due to the presence of residual SO_2 in the flue gas, alkali chloride dust resulting from condensation causes partial conversion into sulphate within the upper section of the boiler [10]. However, it will also form hydrogen chloride, which leaves the boiler as flue gas emission, as seen in the reaction below.

$$2\mathrm{ACl} + \mathrm{SO_2} + \frac{1}{2}\mathrm{O_2} + \mathrm{H_2O} \rightarrow \mathrm{A_2SO_4} + 2\mathrm{HCl} \tag{2.18}$$

As described, in Section 2.2.1, the release of gaseous sulphur to the flue gas is regulated by the temperature in the bed, which subsequently also controls the sulphidity in the flue gas. In addition, the reaction above also implies that the S/Na_2 ratio in the flue gases is a critical parameter concerning chlorine chemistry as well [10]. Figure 2.4 and 2.5 illustrates the principal reactions for sulphur, alkali and chloride, considering the sulphidity in the flue gas is higher or lower than one. Here, the sodium compounds represent the overall alkali contribution, including potassium, where the gaseous alkali entering the flue gas is presented as NaOH, originating from the lower part of the furnace.

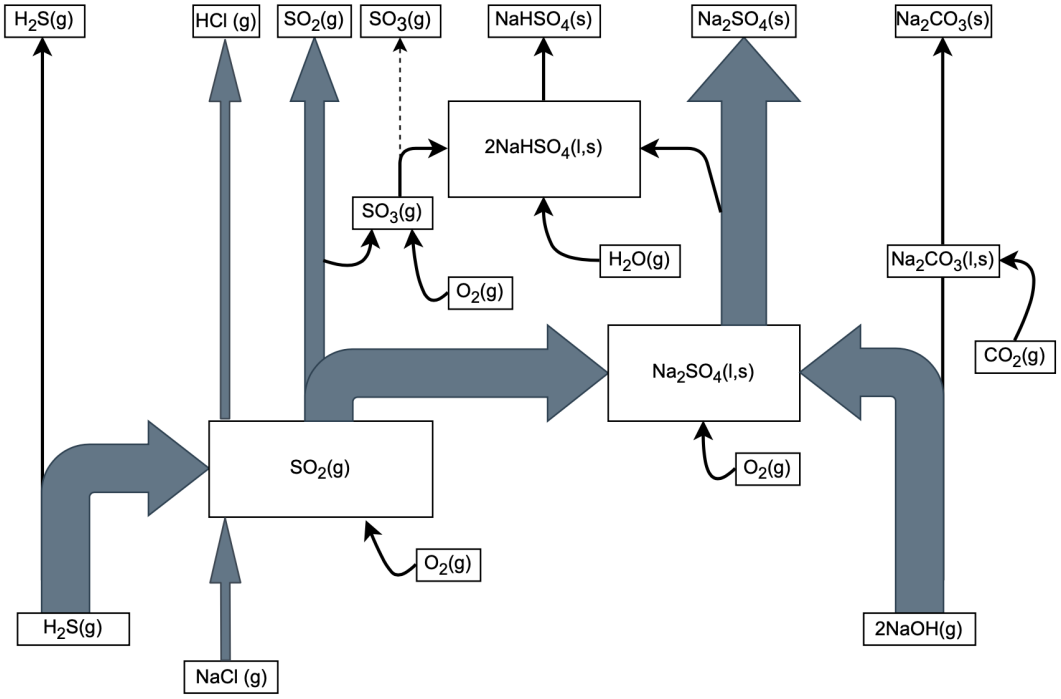

Figure 2.4: Formation routes for sulphur, sodium and chloride in the flue gas. Cool bed: $S/Na_2 > 1$ [10].

In Figure 2.4, a substantial part of the SO_2 is released to the atmosphere, and another substantial part is further oxidised to sulphate which interacts with sodium compounds to form Na_2SO_4 as a particulate. The amount of chlorine released in gaseous form is relatively small. Conversely, the alkali chloride released will undergo almost complete transformation into hydrogen chloride. A minor part of the SO_2 is oxidised to SO_3 of which some is emitted to the atmosphere while some interacts with water and sodium sulphate to form sodium bisulphate dust [10].

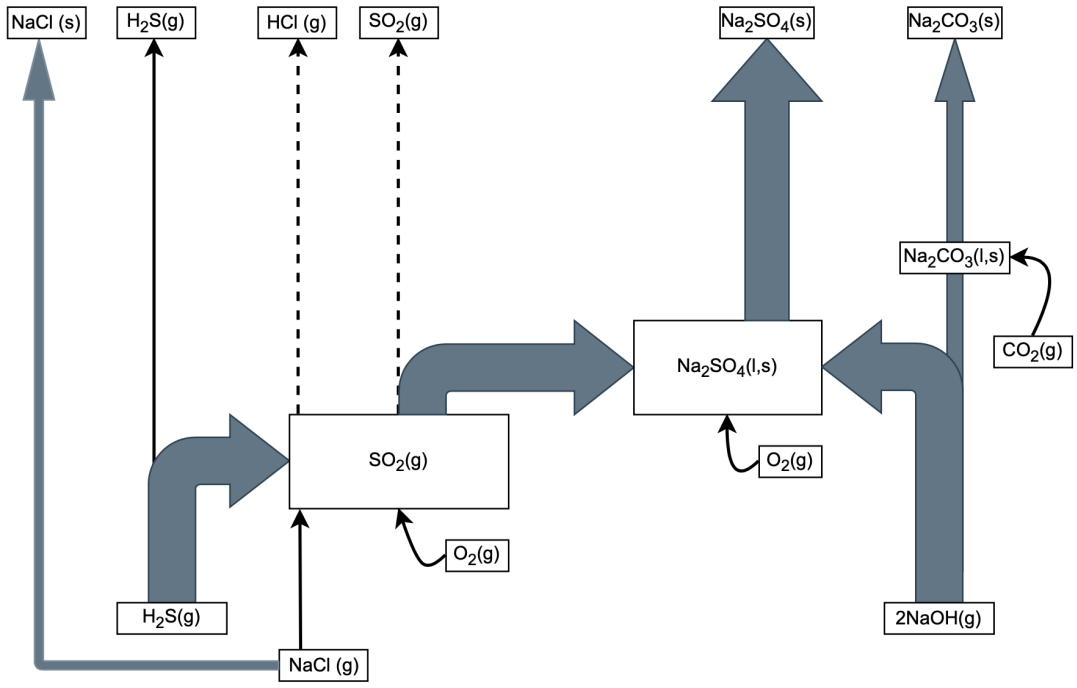

Figure 2.5: Formation routes for sulphur, sodium and chloride in the flue gas. Hot bed: $S/Na_2 < 1$ [10].

In Figure 2.5, the majority of the SO_2 is oxidised to sulphate and interacts with sodium compounds to form $NaSO_4$ with small emissions of SO_2 into the atmosphere. Therefore, a large amount of alkali chloride is vaporised and will not undergo sulphation but instead condenses into alkali chloride dust [10].

To summarise, the SO_x emissions from the recovery boiler are increased by increasing the S/Na_2 ratio in the black liquor as well as lowering the furnace temperature, resulting in a higher S/Na_2 ratio (sulphidity) in the flue gas. Vise versa holds for decreased SO_x emissions, whereas the vaporised sodium compounds bind almost all SO_x in the flue gas into Na_2SO_4 and are recycled back through the ESP [10].

For higher sulphidity in the flue gas, one notice to make is that the formation of acidic sulphate ($NaHSO_4$), see Figure 2.4, contributes to higher fouling and corroding effects inside the furnace. On the other hand, for cases with low sulphidity in the flue gas, the presence of alkali chlorides particulate in the dust also increases the fouling and corrosion tendency as the dust is more prone to sticking on the furnace's walls, see 2.5. This holds especially for the particulate formation of KCl. Alkali chlorides lower the melting temperature range in the dust significantly, resulting in more sticky alkali compounds [10]. Another article suggests that increasing the S/Cl ratio in a combustion system may reduce the formation of alkali chloride deposits, which reduces the corrosion in the furnace. However, the degree of alkali chlorine sulfation is not only dependent on the flue gas composition but also on the temperature, regulating the S/Na_2 ratio in the flue gas [14].

2.2.3 Nitrogen oxides formation routes

Nitrogen oxide emissions, NO_x, commonly refer to the formation of NO, NO_2, and N_2O during combustion, with NO being the most prevalent. The most significant factors of NO_x formation are fuel nitrogen content, oxygen availability, the conversion ratio of fuel-bound nitrogen, temperature, and residence time in the combustion zone [15]. There are 3 main routes of nitrogen formation when using air combustion in the recovery boiler, thermal NO_x, prompt NO_x, and fuel NO_x. An illustration of the different formation routes can be seen in Figure 2.6.

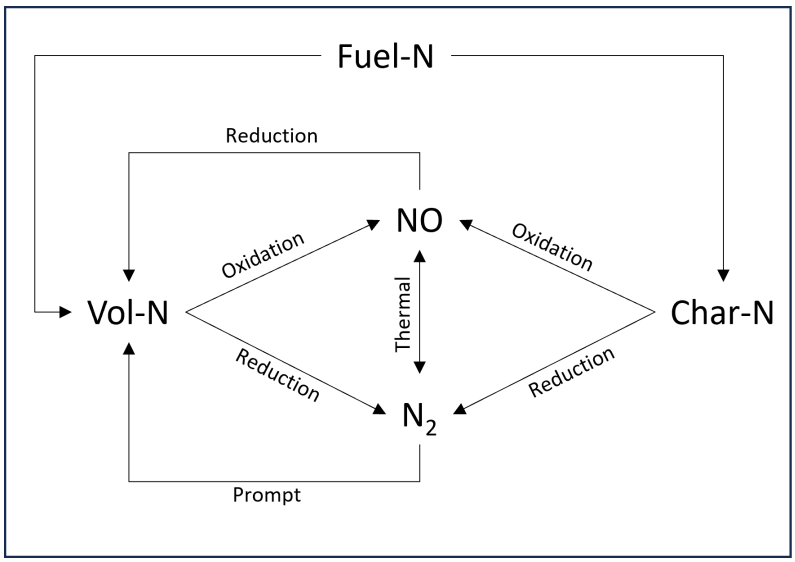

Figure 2.6: Formation routes of thermal, prompt, and fuel NO_x.

Thermal NO_x is primarily formed at high temperatures, around 1350 °C, and can be explained by the Zeldovich mechanism, in Equation 2.19 and 2.20, where N_2 is oxidised by atomic oxygen [16].

$$N_2 + O \rightarrow NO + N \tag{2.19}$$

$$N + O_2 \rightarrow NO + O \tag{2.20}$$

Other factors that affect the formation of thermal NO_x is the flame length due to its effect on the maximum temperature of the flue gas. The contribution of thermal NO_x to total NO_x emissions can vary significantly depending on boiler conditions, particularly temperature. It has been observed that at lower temperatures, approximately 800-900 °C, thermal NO_x constitutes only a minor portion of total NO_x emissions, primarily formed from the oxidation of nitrogen in the combustion air [17]. However, as temperatures exceed 1300 °C, thermal NO_x can become a significant contributor to overall NO_x emissions.

Prompt NO_x is formed during air combustion when N_2 reacts with hydrocarbon radicals. The presence of radicals in the flame zone leads to the formation of hydrogen cyanide (HCN), N and NH according to Equation 2.21 and 2.22, which in turn may form prompt NO_x [16].

$$N_2 + HC \rightarrow HCN + N \tag{2.21}$$

$$N_2 + H_2C \rightarrow HCN + NH \tag{2.22}$$

This occurs almost universally in combustion and since this mechanism requires unburned hydrocarbon fragments it occurs early in the combustion process. However, prompt NO_x is a relatively small portion compared to the total amount of NO_x emissions [16].

The fuel NO_x emissions account for almost all the NO_x emissions in the recovery boiler and originate mainly from the nitrogen in the black liquor, even though the dry black liquor content can contain just up to 0.15 wt% of nitrogen [18]. The black liquor nitrogen is devolatilised when sprayed into the recovery boiler. This devolatilisation, pyrolysis, occurs in the oxidising zone of the recovery boiler which also has been referred to as 'combustion in flight' previously.

In the initial devolatilisation, approximately 2/3 of the nitrogen is released as volatile nitrogen compounds, either N_2 or NH_3. The remaining 1/3 of the total nitrogen is bound in the char carbon matrix, commonly in the form of cyanate (OCN^-) as the sodium compounds in the bed are reduced during the combustion. In general, small portions of nitrogen in the char bed are released forming NO when in contact with oxygen during the reducing phase, but most of this nitrogen exits the recovery boiler along with the green liquor. The cyanate in the green liquor is partly converted into NH_3 when leaving the boiler and entering the dissolving tank. NH_3 in the oxidising zone can either form N_2 or NO. Therefore, the total nitrogen emissions from the recovery boiler are either in the form of NO or N_2 where the share of NO released depends on the operation condition in the recovery boiler. These conditions will be explained further in Section 2.3.1. As the NO reaches the atmosphere, the gas is almost fully converted into NO_2 [17]. A schematic illustration of the black liquor nitrogen formation routes is shown in Figure 2.7

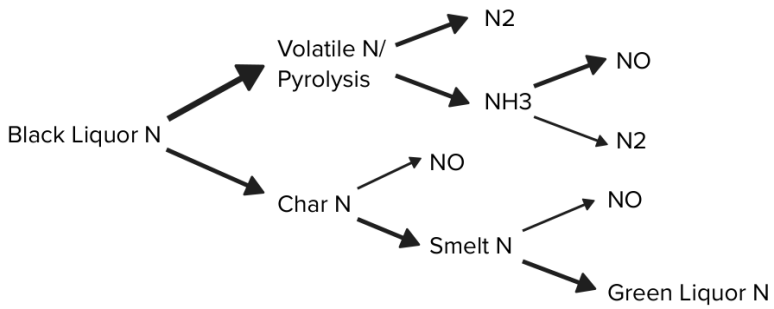

Figure 2.7: Formation routes of fuel NO_x.

2.3 Current BAT and primary control measures of NO_x and SO_x

The current Best Available Technologies (BAT) requirements and an overview of the primary control measures for NO_x and SO_x emission from the recovery boiler will be presented in this section. The control measure techniques are mainly based on the BAT recommendations for power boilers, but the techniques can principally be applied to recovery boilers from kraft pulp mills as well.

As explained in the introduction, requirements for BAT set the standard for emissions to air from kraft recovery boilers in the EU. These emission reference values are presented as ranges due to varying operating conditions among relevant kraft recovery boilers, resulting in higher or lower overall emissions [4]. These ranges are presented in Table 2.1, both as concentration per normal cubic meters of flue gas and kg per ton air-dried mass (ADt). The concentrations are given at standardised reference O_2 content 6 % in flue gas.

Table 2.1: Yearly BAT requirement ranges of emissions for kraft recovery boilers [4].

BAT requirements	mg/Nm^3 at 6 % O_2	kg/ADt
SO_x (as S)	1-100	<0.002 - 0.65
NO_x (as NO_2)	120 - 250	0.73 - 2.0
TRS or H_2S (as S)	0 - 50	0.0007 - 0.40

According to the recommended BAT technologies, for a kraft recovery boiler, emission control within the given ranges is achievable by for example computerised combustion control with good mixing of the black liquor and air while also implementing a staged air system [4]. Other techniques like selective catalytic reduction (SCR) have also been proposed as possible NO_x reduction measures but are seen as emerging technologies and not the best available technology [4]. Moreover, SCR is not considered a primary measure and will therefore not be discussed here.

In recovery boilers, CO concentrations can range from 10 mg CO/Nm^3 to 100 mg CO/Nm^3 on an annual average, with some mills exhibiting even higher levels. However, high CO concentrations pose safety hazards and can also contribute to corrosion of the furnace walls. Currently, there are no BAT requirements specifically addressing CO emissions for recovery boilers. Nevertheless, it remains crucial to maintain a balanced approach, ensuring that both CO and NO_x levels are kept within optimal ranges for a safe operation [4].

2.3.1 Air staging

Air staging is a technique in which NO_x emissions reduction is achieved by introducing two or more combustion zones where the stoichiometric relationship between fuel and air is varied between the zones [12]. For a kraft recovery boiler at stable operating conditions, the black liquor is referred to as the fuel. In a system with four combustion zones, the primary zone would have a substoichiometric relationship between fuel and air to limit the conversion of fuel-bound molecular nitrogen to NO_x as well as limiting the formation of thermal NO_x by lowering the combustion temperature. While in the secondary zone, the relationship between fuel and air is above stoichiometric conditions to achieve burn out of the fuel while also increasing the volume of gas resulting in a lower temperature and limits thermal NO_x formation [16].

Ideally, the hydrocarbons in the black liquor are combusted so that all carbon monoxide is oxidised into carbon dioxide. But, this is not the case for a recovery boiler, where the carbon has to be preserved in the char bed for reduction of Na_2SO_4. To compensate for the incomplete combustion in the lower region of the recovery boiler, tertiary and occasionally quaternary air supply above the pyrolysis zone is necessary to oxidise the remaining CO [16]. Lowering the amount of excess air by regulating air flows will, on the other hand, reduce NO_x emissions since this limits the oxygen available, thereby reducing the amount of fuel-bound nitrogen converted to NO_x and to some extent the formation of thermal NO_x. Finding the optimal distribution of air through all air stages is therefore crucial to maintain low CO emissions while limiting the formation of NO_x [12].

For a conventional kraft recovery boiler, the formation of NO_x originates mainly from NH_3 in the oxidising zone and less from the char bed, as described in Section 2.2.3. Implementing air staging and changing the size of injected black liquor droplets in the spray nozzle are two aspects that have been further investigated by Åbo Akademi University [17]. By making the droplets finer, a larger proportion of the droplets will have time to burn out before reaching the bed surface, resulting in significantly more formation of NO from the char nitrogen. Thus, less nitrogen will be bound to the smelt. Introducing six air stages with coarser droplets will not affect the amount of char nitrogen formed, but instead decrease the formation of NO greatly as the oxidation of NH_3 is limited. The conclusion was that this case in particular formed the least amount of NO. The total formation of NO was significantly higher when combining air staging with finer droplets, but arguably less than for a conventional boiler. Another conclusion was that the NO_x formation decreased as the number of air stages increased, given that the supplied air is distributed more evenly in the recovery boiler. Also, having increased temperatures ranging from 800 °C to 1000 °C in the oxidising zones increased the formation of NO significantly [17].

2.3.2 Ammonia injection

Another method that has been reported for the reduction of NO_x emissions is to inject ammonia diluted in water, into the recovery boiler. By adding NH_3 to the exhaust gas as an active reducing agent, the present nitrogen oxides can be converted into N_2.

$$4\,NO + 4\,NH_3 + O_2 \rightarrow 4\,N_2 + 6\,H_2O \tag{2.23}$$

For this selective non-catalytic reduction (SNCR) to work properly, the NH_3 has to be dosed in an above-stoichiometric ratio in relation to the continuously measured NO_x target value. The amount injected should be somewhere between 2.1-3.3 mol NH_3 or 1.1-1.6 mol urea per mol NO_x. The performance of this process is strongly dependent on the mixing conditions between the ammonia and NO_x in the exhaust gas. The reduction reaction is also dependent on an optimal temperature interval in the boiler. Injecting ammonia at temperatures below 900 °C results in lower conversion and fewer portions of NH_3 will leave the boiler unreacted, so-called 'ammonia slip'. At higher temperatures, above 1000 °C, the oxidation of NH_3 into NO_x is increased [12].

This SNCR method has successfully been used in power boilers and bark boilers, but the applicability of this in recovery boilers has not been investigated as much. However, one study has shown that injection of ammonia into a recovery boiler with a spruce-based black liquor load of 132 ADt/day gave a reduction of NO_x up to 30 %. A solution of 10-11 % ammonia water was injected into the chamber at 910-920 °C. The dosage was 50 l/h which corresponded to approximately 1.5 ml of NH_3/Nm^3 exhaust gas. At the given dosage, the results showed that no relevant ammonia slip was determined. One difficulty in using this type of SNCR is the varying temperature zones in the recovery boiler and it is still unclear where the injection ports should be placed for the most efficient results, especially when the recovery boiler load is altered. Improvements to the ammonia injection system can be made by having an adequate number of injection ports for increased penetration and mixing conditions with the exhaust gas. Having sufficient residence time for ammonia to react is also a crucial aspect [12].

Tests with SNCR for NO_x reduction in a kraft recovery boiler have also been carried out by Metso Power based on a 2000 ADt/day recovery boiler built in the year 2001. The amount injected varied between 0.8-1.7 mol NH_3 per mol NO_x depending on load ranges over 60 – 100 %. At full operating load, the $NH_3/NO_{initial}$ ratio was 1.3 and there were four injection points just below the nose of the boiler, above the quaternary airports. The results showed a reduction of NO_x for all cases, where a 45 % reduction at full load was achieved with limited ammonia slip (17.5 NH_3 slip mg/Nm^3) and no or only a minor impact of other emissions. It was stated in the study that it was hard to reveal any trends between the $NH_3/NO_{initial}$ ratio and the reduction. One explanation could be that the rate of reduction is heavily dependent on conditions in the injection region. For example, the temperature differed from 830 °C to 925 °C upon measurement at the injection region [19].

There are some safety hazards associated with ammonia injection. Managing ammonia slip is complicated due to limited feedback for reagent control, as well as challenges in determining optimal placement. Furthermore, SNCR systems in bark boilers face difficulties with rapid load changes, leading to variable NO_x reduction effectiveness and unstable performance under fluctuating operational conditions. Another potential hazard arises from unreacted ammonia reacting with SO_3 to produce ammonium bisulphate, which can precipitate at air heater temperatures, causing fouling and potential plugging [12].

It can also be safety risks when injecting water into a recovery boiler. If the water comes into contact with the smelt, an explosion can occur. This may be due to the rapid conversion of water into vapour with a very large volume or to the decomposition of water into hydrogen and oxygen, which then ignites. It is therefore important that the water is evaporated before it reaches the smelt [20].

2.3.3 Flue gas recirculation, fuel staging and reduced air preheat

Flue gas recirculation is a technique in which NO_x formation is reduced by recirculating flue gas into the combustion zone. This limits oxygen availability while also reducing the temperature of the flame, which reduces the conversion of fuel-bound NO_x and the formation of thermal NO_x [12].

Fuel staging is a technique similar to air staging in which the stoichiometric relationship between fuel and air is altered. The objective of this technique is, contrary to air staging, not to limit the formation of NO_x, but rather to support the conversion of formed NO_x back to molecular nitrogen. This is done through the creation of three combustion zones, in the primary zone a majority of the fuel is burnt out with excess air. In the secondary zone, more fuel is added which creates a substoichiometric atmosphere in which hydrocarbon radicals are formed which in turn react with NO_x and reduce the NO_x back to molecular nitrogen. The combustion of the fuel is then completed in the third zone by supplying excess air [12].

Other measures that can be taken to reduce NO_x emissions are combustion with reduced air preheat temperature, water injection, and installing low NO_x burners [12]. Reducing the air preheat or injecting water into the recovery boiler reduces the flame temperature and thereby reduces the amount of thermal NO_x formed [12]. Low NO_x burners apply the principles of either, air staging, flue gas recirculation, fuel staging, or a combination of the three mentioned techniques to achieve reduced NO_x emissions [12].

2.3.4 Primary control measures for SO_x

The recommended BAT measures for SO_x removal from the recovery boiler is to increase the dry solid content and/or decrease the sulphidity of the black liquor. Increasing the dry solid content of black liquor reduces the SO_x emissions by increasing the temperature in the furnace. As described earlier in Section 2.2.2, higher temperatures in the bed limit the release of gaseous sulphur and therefore reduces the sulphidity in the flue gas, resulting in lower SO_2 emissions. This allows more sulphur to react with sodium in the bed to form Na_2CO_3. There are, however, some adverse effects of increasing the dry solid content as higher temperatures might cause increased emissions of NO_x. Decreasing the sulphidity of the black liquor ensures that a majority of sulphur present can react with sodium, limiting the amount of SO_x that can be formed [4].

2.4 Wet flue gas treatment with NO oxidation

A study on the coabsorption of SO_x and NO_x techniques, with NO oxidation from a gas-fired furnace flue gas, was done through technical-scale experiments and simulations. The study indicated that the technique can achieve >90 % NO_x removal with > 99 % SO_x removal. In this technique, an oxidative agent such as O_3, H_2O_2 or ClO_2 is used to oxidise NO to NO_2 is injected into the flue gas to make the nitrogen soluble in water. SO_2 is adsorbed spontaneously to water with solubility being limiting. When dissolved, SO_2 reacts with water to form bisulphite which forms sulphite through a dissociative equilibrium reaction which is weighted towards sulphite under alkaline conditions. Sulphite then interacts with the dissolved NO_2 through hydralisation which takes place at a comparable rate to that of SO_2 absorption to water. This allows for efficient co-removal of NO_x and SO_x in a wet scrubber like equipment used for SO_x removal [21].

This method is heavily dependent on the coexistence of sulphur and nitrogen in the flue gas to achieve high removal efficiency. In the case of combustion of sulphur deficient fuel, Na_2SO_3 can be added in the scrubber liquid to increase the removal efficiency, however, this is associated with increased operational cost [21]. One potential way to reduce the amount additional Na_2SO_3 to the scrubber liquid could be recycling the scrubber effluent back to the recover boiler. This has been investigated in a 25 MW_{th} waste-to-energy power plant. In the study, it was found that recirculating the scrubber effluent would reduce the NO_x formation by the addition of nitrites and it is also discussed that recirculated sulphates from the effluent can be reduced to SO_2 by alkali sulphate decomposition under the right circumstances [14].

However, no increase of SO_2 in the flue gas was observed during the experiment which can be attributed to the temperature being too low or the environment not being reducing enough to achieve decomposition at the point of injection. If decomposition of alkali sulphates can be achieved, recirculation of scrubber effluent might be an efficient way to reduce the operational cost of the equipment as it lowers the formation of NO_x. This would, in turn, reduce the amount of sulphite needed for absorption while also increasing the SO_2 content in the flue gas, thereby decreasing the amount of Na_2SO_3 needed to be supplied to the absorption liquid. Another benefit is that if the scrubber effluent can be recirculated to the recovery boiler, it will decrease the amount of effluent that has to pass through the wastewater treatment [14]. Ideally, implementation of the scrubber would mean that a sulphur cycle would be possible to introduce to the kraft process as depicted in Figure 2.8.

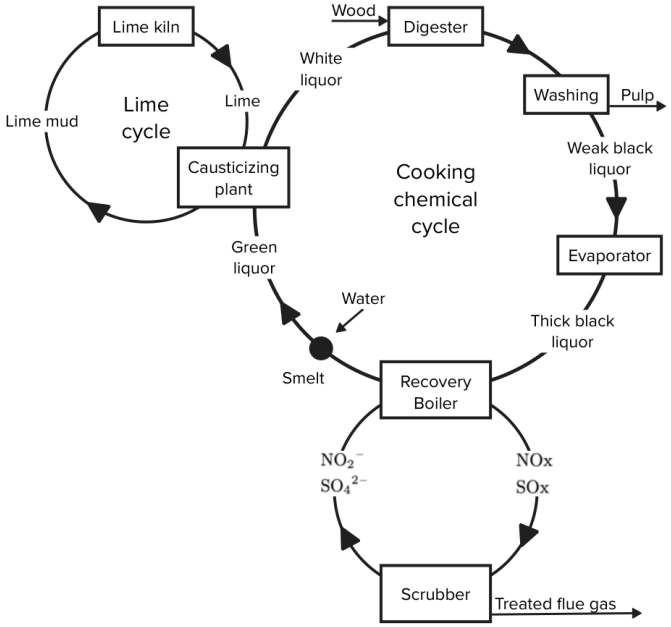

Figure 2.8: The kraft recovery process with recycling of scrubber effluent.

3

Method

The method of this work is illustrated by a methodology flowchart, shown in Figure 3.1. The literature study provides theory of the recovery boiler and its chemistry. Data collection took place at Södra in Mönsterås, involving interviews, plant tours, and data gathering.

The recovery boiler is modeled based on the collected data using Aspen Plus V14. The software was chosen for its capability to simulate mass and energy balances under defined conditions and handle unconventional materials like black liquor.

Data processing and modelling of the recovery boiler involved iterative adjustments based on data insertion, assumptions, simulation runs, and troubleshooting. Improvements to the model were performed based on input and output control values. The model was validated by comparing simulated results in Aspen Plus with Södra's data and the literature through mass and energy balances in Excel, followed by a sensitivity analysis of the finalised base case model.

Primary reduction measures were incorporated into the model and were assessed through changes in the mass and energy balances and some key performance indicators (KPIs). Despite limitations in reaction kinetics, the model provided insights into the effects of different measures on emissions, aiding the discussion.

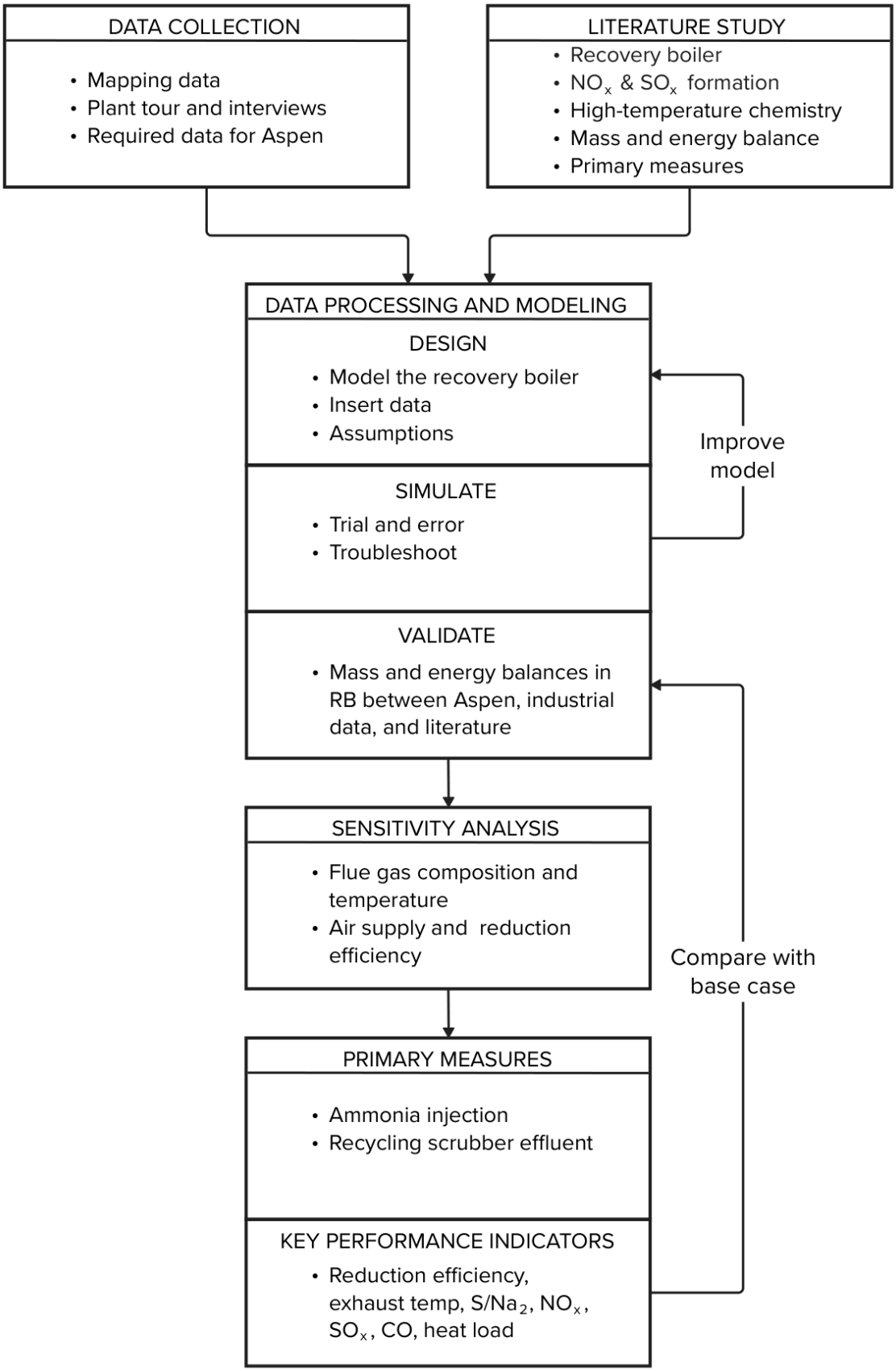

Figure 3.1: Methodology flowchart for this thesis.

3.1 Collecting plant data

The data presented in this section were collected from the process at Södra Cell Mönsterås. Both internal and external measurements and reported data were provided under stable and normal operating conditions. Although certain data was sourced from 2022, it remains applicable as there have been no changes in the operation of the boiler since that time. Collecting all relevant data during the visit and getting familiar with the different inlet and outlet streams regarding the recovery boiler was of great importance for modelling accurately.

3.1.1 Södra's recovery boiler

Figure 3.2 presents a simplified flowchart of the recovery boiler at Södra Cell Mönsterås. It illustrates the pathway of the flue gases through the boiler, followed by entry into the ESP. Here, a portion exits as exhaust gases through the chimney, while the remainder is recirculated as dust. The dust is subsequently blended with weak black liquor before being evaporated with make-up. This results in thick black liquor entering the recovery boiler just above the secondary air. Additionally, the flowchart indicates the entry points for all air injections, as well as the CNCG and DNCG. Furthermore, it shows the locations of feedwater injection and steam exit from the boiler.

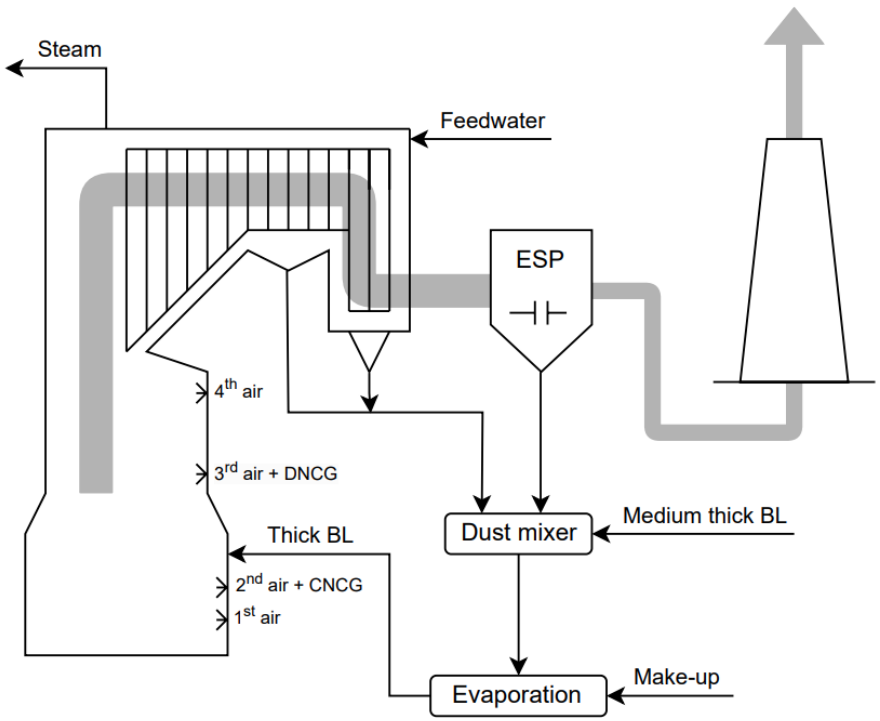

Figure 3.2: Schematic flowchart of the recovery boiler at Södra Cell Mönsterås.

3.1.2 Inlet data

The pulp produced at the site is mostly spruce and pine-based timber. Therefore, only data regarding softwood-based black liquor was collected. Table 3.1 shows the yearly average elemental composition of the black liquor from laboratory tests, the lower heating value (LHV), and its S/Na_2 ratio. The sample was taken just before the black liquor was sprayed into the boiler, which includes the Electrostatic Precipitator (ESP) dust and make-up chemicals to the total composition.

Table 3.1: Elemental composition of thick black liquor (dry basis) [22].

C wt%	H wt%	O wt%	N wt%	S wt%	Na wt%	K wt%	Cl wt%	S/Na_2 mol%	LHV MJ/kg
31.4	3.71	37.74	0.06	4.59	20.34	2.0	0.16	0.32	12.45

Other inlet data was collected from a previous design specification study performed on Södra's recovery boiler. Since the design specification study also provided necessary outlet data for the boiler, the study was partly used as a reference case when running the Aspen model with the corresponding input data. The study assumed a guaranteed liquor load of 4330 ton dry liquor per day (75 % dry solids content). Table 3.2 shows the inlet rates and temperatures of black liquor feed and air supply entering the boiler, where the diluted non-condensable gas (DNCG) was assumed to have the same composition as air. The flow and temperature of feedwater for steam production in the recovery boiler are also presented in Table 3.2.

Table 3.2: Inlet flows and temperatures [20].

Inlet	Flows	Temp [°C]
Black liquor feed [kg/s]	66.82	141
Feedwater for steam [kg/s]	174.0	124
Primrary air [Nm^3/s]	47.71	165
Secondary air [Nm^3/s]	59.80	165
Tertiary air [Nm^3/s]	11.01	30.0
DNCG [Nm^3/s]	11.90	90.0
Quaternary air [Nm^3/s]	31.98	30.0
Total air [Nm^3/s]	162.4	

On site, before the black liquor enters the boiler, volatile organic compounds (VOCs) are released from heating and pressurising the black liquor in the evaporator steps. Along with methanol, a series of sulphurous gases are also formed under these conditions, mainly H_2S, methyl-mercaptan (MM), dimethyl sulphide (DMS), and dimethyl disulphide (DMDS). These concentrated non-condensable gases (CNCGs) are then injected into the recovery boiler, where the gas is combusted. In Table 3.3, the calculated mass flows of CNCG compounds entering the boiler are listed, based on data from 2022-04-27, when the daily production was 2200 ADt, which is the desired production rate.

Table 3.3: CNCG inlet flows and temperature [20].

Compound		Units
H_2S	7.5	g/s
MM (CH_4S)	60	g/s
DMS (C_2H_6S)	35	g/s
DMDS ($C_2H_6S_2$)	1.7	g/s
Methanol	52	g/s
Total flow	0.16	kg/s
Temperature	84	℃

3.1.3 Reference data

Collecting relevant reference data was essential for comparison with the results from the Aspen simulations. Data from the design specification study provided insights into how the temperature was distributed in the boiler and what target temperatures were reasonable for each process operation in Aspen. These data are listed in Table 3.4, where the values were calculated between the air stages inside the recovery boiler. Table 3.4 also shows the compositions of O_2 and CO provided by the same study in these regions.

Table 3.4: Distribution of temperatures and O_2 in the boiler based on design specifications [20].

Region	Temp [°C]	O_2 dry [mol%]
Between primary and secondary	1596	1.6
Between secondary and tertiary	1455	0.0
Above tertiary	1301	0.7
Above quaternary	1084	3.1
Nose level	1096	2.5

The monthly average concentrations of sodium compounds in the smelt from Södra's recovery boiler are presented in Table 3.5 (2024-03). The green liquor sample was dissolved in weak liquor prior to the measurement. Based on the total titratable alkali (TTA) and each compound concentration, the weight percentages were calculated, assuming that the compounds presented in the table were the only ones present in the smelt. The reduction efficiency (RE) was approximately 94 % during the measurement period.

Table 3.5: Concentrations and compositions of dissolved green liquor [22].

Smelt compound	g/l	wt%
Na_2S	52.0	31.5
Na_2CO_3	110	66.5
Na_2SO_4	3.31	2.00
TTA	168	100

Södra's flue gas composition was measured by two consulting companies, 'DGE' and 'ILEMA Miljöanalys AB', in February 2023 and 2019, respectively. DGE conducted their measurements over a single day, while ILEMA's measurements were taken over three days. However, both were conducted with the measurement point located inside the chimney of the recovery boiler. The load was approximately 4000 tons of dry liquor per day during the measurements. Some of these flue gas species are listed in Table 3.6, along with the measured flue gas flows and temperatures. The flow and average compositions by volume percentage presented in the table were calculated on a wet gas basis. It should also be noted that the CO levels were higher at times during the measurement period, exceeding 1000 ppmv at most. Therefore, the level of CO is presented as an acceptable range due to frequent fluctuations during the measurements.

Table 3.6: Measured flue gas data carried out by DGE and ILEMA [20].

Flue gas data	DGE	ILEMA	Units
O_2	3.10	2.45	vol%
H_2O	18.4	20.9	vol%
CO_2	10.3	12.7	vol%
CO	100 - 500	150-550	ppmv
NO_x (as NO_2)	70.0	-	ppmv
SO_x (as SO_2)	< 1.00	-	ppmv
HCl	< 2.50	-	ppmv
Flue gas flow	241.7	220.1	Nm^3/s
Flue gas flow dry	197.3	173.9	Nm^3/s
Flue gas temperature	195.1	200.1	℃

The reported yearly emission data for sulphur and NO_x emissions from the recovery boiler were also provided in Södra's environmental report (2023), as shown in Table 3.7. The concentration levels are given at a standardised reference O_2 content of 6 % in flue gas for softwood, and the values are comparable to the BAT requirements from Table 2.1.

Table 3.7: Yearly emission values from Södra's recovery boiler compared to BAT requirements [22].

Södra Cell Mönsterås	Södra mg/Nm^3	Södra kg/ADt	BAT mg/Nm^3	BAT kg/ADt
SO_x (as S)	0	0	1-100	<0.002 - 0.65
NO_x (as NO_2)	141	1.10	120 - 250	0.73 - 2.0
TRS or H_2S (as S)	-	0.10	0 - 50	0.0007 - 0.40

Relevant data regarding steam generation were provided for the period 2024-03, as shown in Table 3.8. The values were obtained from Södra's real-time measurement data, where the heat-to-steam and total heat input to the boiler are calculated values based on the mass and energy module of the recovery boiler.

Table 3.8: Reference data for steam generation [22].

Steam Generation		Units
Steam production	174	kg/s
Steam temperature	480	℃
Steam pressure	61.0	bar
Heat load to steam	460	MW
Total heat load input to boiler	637	MW

3.2 Process modelling

The recovery boiler was modeled in a similar way as described in Section 2.2, by dividing it into different parts. Additionally, to model this complex chemical process, some assumptions were made to simplify the recovery boiler.

3.2.1 Assumptions and thermodynamic model

The modelling of the recovery boiler was based on certain assumptions. These assumptions, derived from a literature review, are listed below [9].

- The process is kinetic-free and operates at steady-state conditions.
- The model is zero-dimensional, with output variables generated based on input variables.
- The model only considers chemical and thermodynamic equilibrium.
- The recovery boiler operates at 1 bar.
- N_2 was considered as inert in the RGibbs reactors.
- Dust formation in the boiler was not considered.

The thermodynamic model used for this design was the Peng Robinson-Boston Mathias (PR-BM) equation of state, employed to compute the properties of various components throughout the entire process. This combination of the Peng Robinson and Boston Mathias equations makes it suitable for both pyrolysis and gasification of biomass, as it can handle hydrocarbons and light gases [9] [23].

3.2.2 Design specifications of the model

The initial goal of modelling the recovery boiler in Aspen was to match the mass and energy balances with Södra's industrial data. The recovery boiler functions as a chemical reactor, facilitating the recovery of inorganic compounds as smelt. Due to the intricate nature of black liquor combustion within recovery boilers, the model only incorporated the crucial steps of this process. This section will specify each part of the journey of black liquor and volatiles through the recovery boiler in the model. Figure 3.3 provides an overview of the model structure and outlines the different simulation sections as hierarchy blocks.

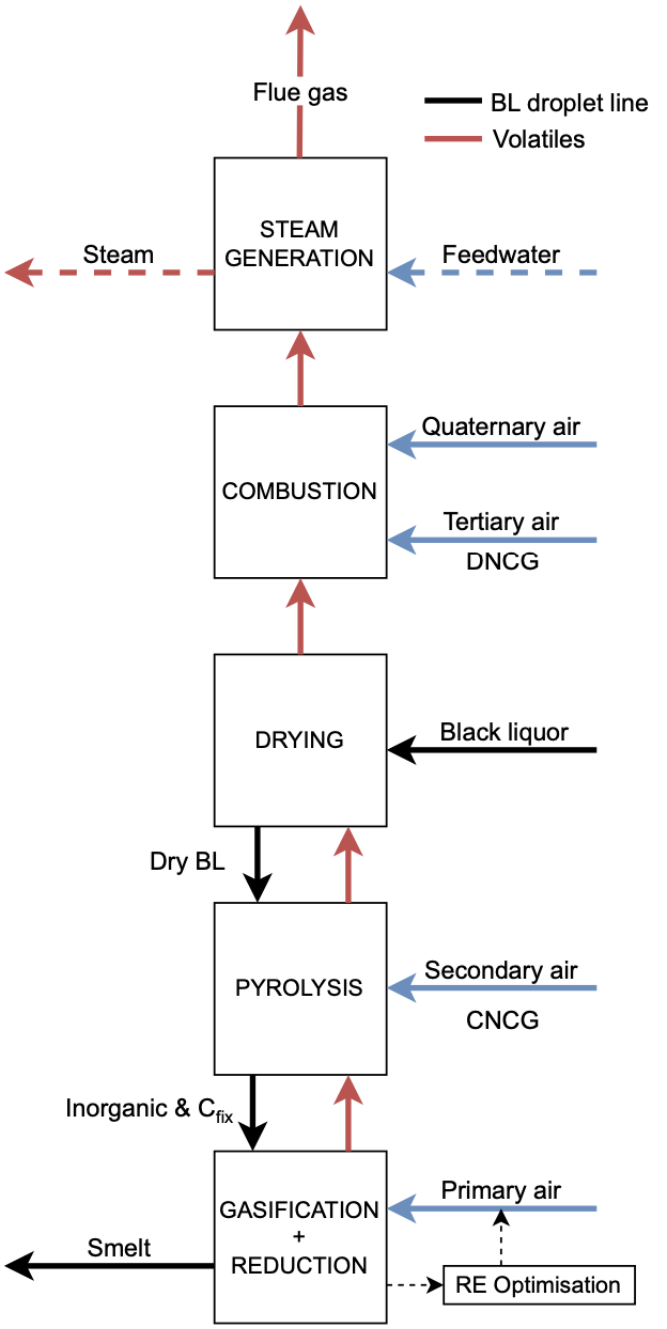

Figure 3.3: An overview of the recovery boiler modelling structure.

To clarify, the thick black line is the path of the black liquor solids through the recovery boiler going downstream, where part of it ends up in the smelt, and the red lines represent the flow of the volatiles going upstream, exiting the boiler as flue gas. The blue lines are the different air flows into the boiler, with CNCG and DNCG added at corresponding air levels. The dashed blue line represents the inlet of the feedwater entering the steam generation section and exiting as steam (dashed red line). Figure 3.4 to 3.8 will further illustrate in depth how the model was constructed for each hierarchy block.

To facilitate the properties of the black liquor in Aspen, the liquor was defined as a non-conventional solid. The compositions from Table 3.1 were inserted into the ultimate analysis. Since the inorganic compounds could not be inserted into this analysis, Na and K were defined as conventional solids. To ensure a component fraction of 1 for the ultimate analysis, the fractions were divided with a normalisation factor of 0.7766, which refers to the difference between the total composition and the fraction of the inorganic compounds. Since the compositions in Table 3.1 are calculated on a dry basis, the moisture content had to be defined in the non-conventional proximate analysis.

The first step was to model the drying section, shown in Figure 3.4. The inlet stream of black liquor enters the RStoic unit (DRYING) to simulate the drying process by using stoichiometry reaction modelling. The black liquor particles were then exposed to volatiles from the lower part of the boiler (V7), which caused the rest of the moisture to evaporate.

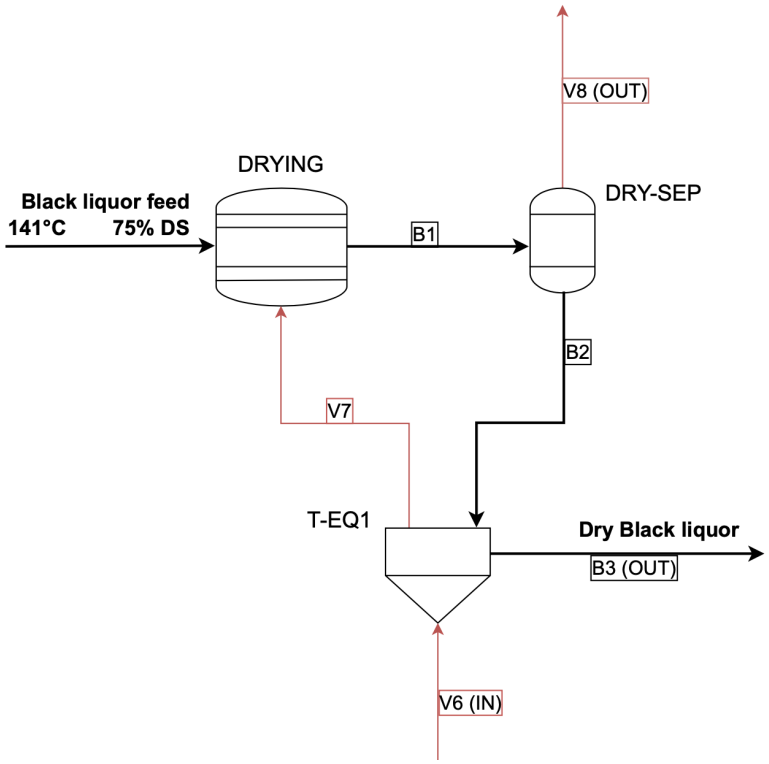

Figure 3.4: Process flow diagram of the drying section, where the wet black liquor (B) entering the boiler and is completely dried by volatiles (V) traveling upwards.

Given that black liquor was considered a non-conventional component, Aspen assumed its molar mass to be 1 g/mol. With the molar mass of water being 18.02 g/mol, the stoichiometry of the reaction indicated that 1 mol of wet black liquor reacts to produce 0.055 mol of water. Equation 3.1, therefore, displays the evaporation of moisture that simulated the drying extent in the RStoic.

$$\text{Wet Black Liquor} \rightarrow 0.055\,H_2O \tag{3.1}$$

It was assumed in this model that post-drying, the black liquor became entirely dry. After that, the DRY-SEP unit separated the formed water vapor (V8) and the dry black liquor droplets (B2). The SSplit unit (T-EQ1) ensured thermal equilibrium between the dry black liquor, transitioning to the pyrolysis section, and the volatiles originating from the lower part of the boiler (V6).

Figure 3.5 illustrates the course of events for the dry black liquor, entering the pyrolysis region. The liquor was mixed with volatiles (V1) from the reduction section through the T-EQ2 before entering the DECOMP unit. Here, the non-conventional components in the liquor were decomposed into a homogeneous mixture of the elemental substances C, H_2, N_2, Cl_2, S, O_2, H_2O, and ash. The DECOMP unit is based on the RYield model where the yields had to be specified based on the black liquor ultimate analysis. Since the inorganic solids (compounds of Na and K) were present in the black liquor but not decomposed, the yields based on the ultimate analysis were multiplied by the normalisation factor before being specified in the RYield model. Summing up all yield fractions, including the inorganic fraction, resulted in a total yield of 1.

The black liquor then entered the PYRO-REA unit which was based on the RGibbs model that performed the pyrolysis, see Figure 3.5. This model uses Gibbs free energy minimisation method to determine the distribution and composition of the multi-phase mixture, whereas mass and energy balances were coupled based on additional incoming streams of CNCG, volatiles from the reduction section (V2), and secondary air. The purpose of splitting the secondary air (SEC-SPLIT) was to ensure incomplete combustion of carbon in the PYRO-REA unit by limiting the oxygen available. Besides the volatiles released during pyrolysis, described in Section 2.2, the inorganic salts together with the fixed carbon were separated by the PYRO-SEP unit, exiting the pyrolysis zone (B7). The PYRO-SEP unit continued to drive all released volatiles upward in the boiler where the rest of the secondary air was used to oxidise more of the combustion gases through the FLAME unit (RGibbs), especially CO.

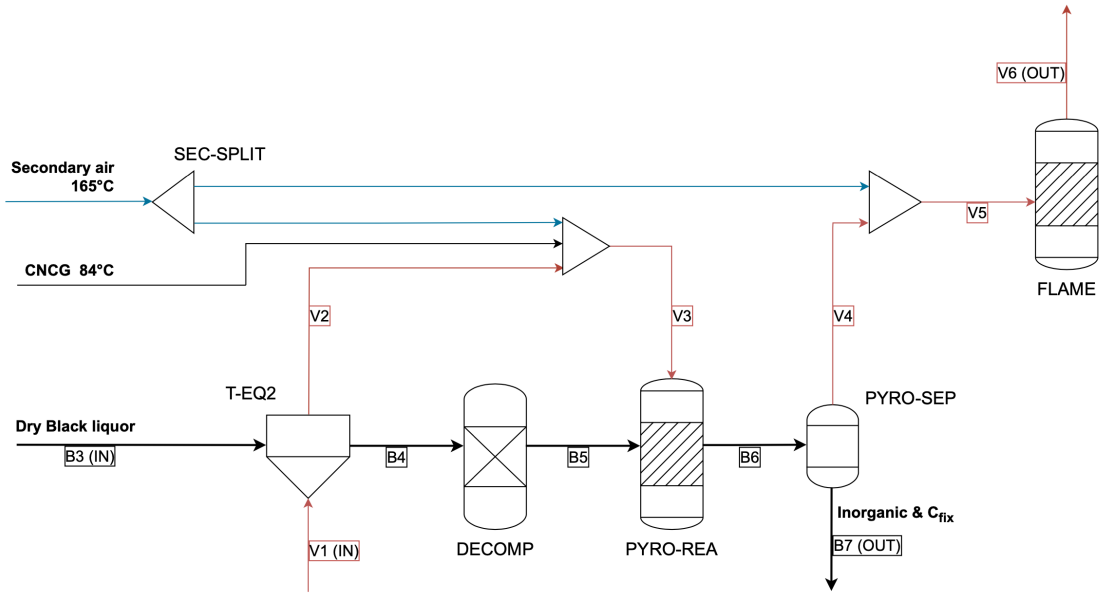

Figure 3.5: Process flow diagram of the pyrolysis section, where the dry black liquor is decomposed into volatiles, inorganic compounds and fixed carbon. The volatiles traveling upwards through the pyrolysis section are combusted in the FLAME unit with secondary air.

After the pyrolysis of the dry black liquor droplets, the inorganic porous particulate material and the fixed carbon reacted together with the primary air in the RGibbs reactor (GAS & RED). The main gasification reactions that occurred is shown in Equation 2.6 to 2.9. These reactions provided the necessary energy for the endothermic reactions to take place in the reduction zone, described in Equation 2.10 to 2.12. Achieving high reduction efficiency in the smelt depends on preventing reoxidation of Na_2S to Na_2SO_4. Thus, maintaining an oxygen-deficient environment is crucial for this process.

To achieve this, an optimisation tool was used to iterate the necessary amount of primary air required to minimise the deviation between the simulated and targeted reduction efficiency (RE). Equation 2.13 was used to achieve this while the primary air served as the model output, which could be utilised for model validation. The last step was to separate the formed volatiles (V1) and the smelt, mainly composed of Na_2CO_3, Na_2SO_4, and Na_2S, in the char bed region.

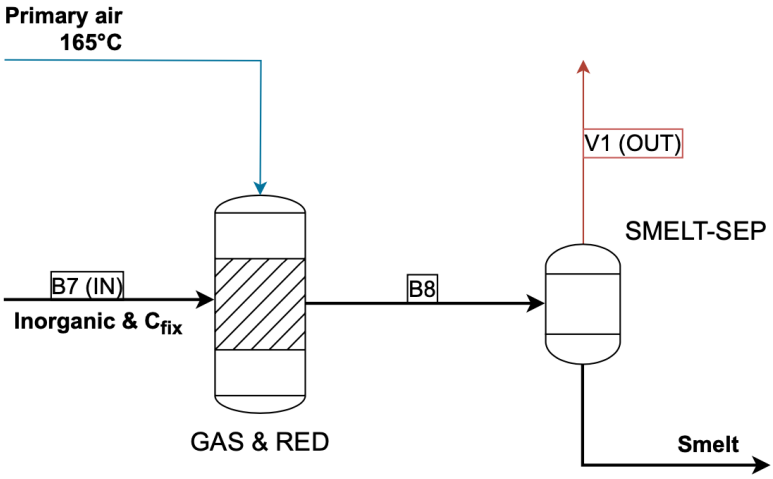

Figure 3.6: Process flow diagram of the gasification and reduction section. The primary air provides the optimal amount of oxygen for gasification and reduction, resulting in release of volatiles (V1) and a smelt leaving the boiler.

The gases produced from the gasification in the lower part of the boiler then continued to the pyrolysis section to be combusted with secondary air. Since the burning process may not be complete, extra combustion was needed to burn any remaining carbon monoxide and sulphur gases. Figure 3.7 illustrates the additional tertiary and quaternary air that entered the two RGibbs unit for combustion (COMB1 and COMB2). A stream of dilute non-condensable gases (DNCG) was injected into COMB1 to imitate the real process.

The tertiary and quaternary air flow was also optimised for additional combustion to reduce overall emissions, where the quaternary air was further aiding in reducing unwanted pollutants. After the combustion zone, the flue gas continues to travel towards the steam generation higher up in the recovery boiler, where the heat released from the flue gas was utilised to produce steam.

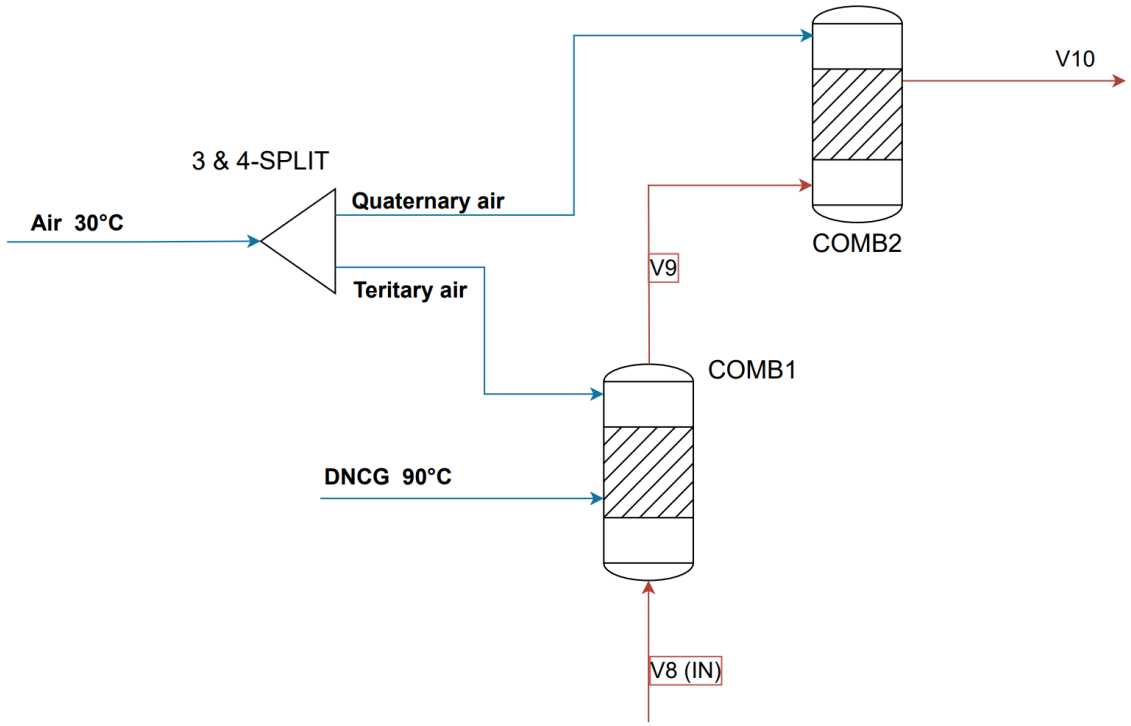

Figure 3.7: Process flow diagram of the combustion section (above pyrolysis). Flue gases in the volatile stream are combusted with DNCG, tertiary air and quaternary air.

The steam generation occurs in the upper section of the recovery boiler, where the liquid feedwater is transformed into super-heated, high-pressure steam. This convective heat transfer is achieved through the exchange of heat between the flue gases and the water-steam system. Figure 3.8 describes the steam generation process in the model. The dashed blue line represents the feedwater entering the boiler while the dashed red line represents the steam produced. Additionally, the solid red lines indicate the path of the flue gas.

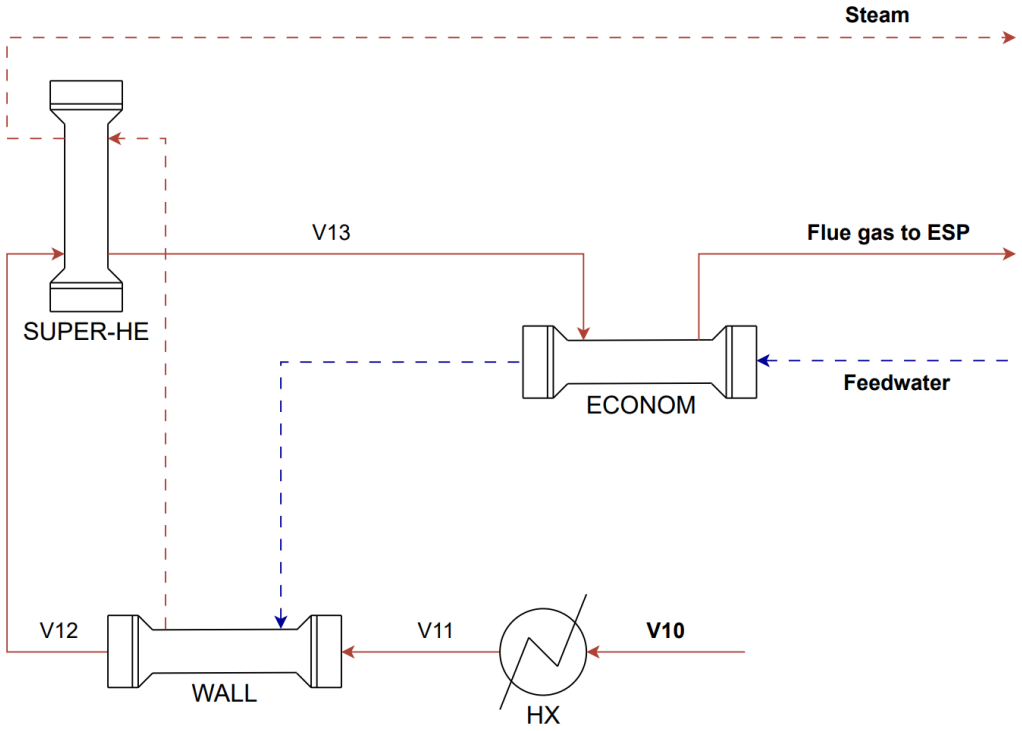

Figure 3.8: Process flow diagram of the steam generation section. The flue gas (red line) exchanges heat to the steam-water system (dashed line) before leaving the boiler.

In comparison to real steam generation, where the heat formed is captured by tube wall heat exchangers along the boiler and then used to heat up the steam, this process is a bit simplified but uses the same idea. In order to imitate the heat exchanger tubes, heat from all the different sections was 'taken' to achieve the same temperatures as the design specification of the boiler (Table 3.4) and was then inserted into a heat exchanger (HX). By doing this, the volatiles were heated to the design specific temperatures before entering the heat exchanger (WALL) which represents all the heat transfer from all tubes.

Therefore, as the gases ascend, they undergo heat exchange with the furnace walls, in the WALL unit. Subsequently, the gases then proceed even higher in the furnace, entering the super-heater (SUPER-HE), where the saturated steam is super-heated. Lastly, the gases flow into the economiser (ECONOM), where the liquid feedwater undergoes preheating, before exiting the boiler.

Since the model uses equilibrium-based reactors, the amount of CO in the flue gas was below 1 ppmv due to complete combustion and mixing in the RGibbs reactors. However, this is not the case in Södra's recovery boiler, therefore, to match the level of CO for better validation results, the temperature was increased in the last combustion reactor (COMB2), see Figure 4.4. Since no reactions occurred after the COMB2 reactor, the composition in the flue gas stream was not affected by the temperature decrease in the steam generation section.

3.3 Model validation

To validate the model, mass and energy balances were calculated in Excel according to a literature study [16], based on relevant industrial data collected and used as input for the calculations. The results from the balances were then compared with the simulated result from Aspen as well as the reference data from Södra's recovery boiler.

The main assumptions and considerations made during the mass and energy balance calculations were:

- The calculated mass flows were based on 50.115 kg of black liquor solids (BLS), referred to as the total black liquor inlet flow of 66.82 kg/s.
- The air flows and flue gas mixture were assumed to be ideal when calculating normal volumetric flows (Nm^3/s at 0 °C and 1 atm).
- The carbon content in the smelt was 1 wt% of the total smelt.
- When calculating the carbon and sulphur losses in the flue gas, mean values of CO and SO_x (dry basis) from the DGE measurement (see Table 3.6) were used. The TRS flow in the flue gas stack was obtained from Södra's environmental report (see Table 3.7).
- It was assumed that 10 wt% of the initial sodium would end up in the dust recycle.
- The particulate loading was 0.0002 kg/Nm^3 dry flue gas in stack.
- The steam generation was assumed to have no mass losses (water in was equal to steam out). Blowdown and sootblowing steam flows were also neglected.
- Radiation losses were 0.3 % of the total heat input.
- Unassociated losses were estimated to be 1.5 % of the total heat input.

All comparisons for the validation will be shown in Section 4.1 and the calculations can be seen in Appendix A.

A sensitivity analysis of the base case model was performed as part of the validation to verify the stability of the model, as well as finding correlations between key performance indicators such as the composition and temperatures in the upper part of the furnace. Effects on the reduction efficiency and flue gas temperature were also investigated by altering the primary and secondary air flows for the base case model within reasonable operating conditions. The deviations provided from the analysis were plotted and presented in the results.

3.4 Implementation of primary measures

3.4.1 Ammonia injection

Considering the results from the 2000 ADt/day kraft pulp mill study on water-diluted ammonia injection into a recovery boiler (see Section 2.3.2), a similar implementation was investigated in this work. This was done using the given specifications from the study as input data in the model, including the reduction rate of NO_x that was 45 %, and calculating the mass flows of water and ammonia based on the initial NO_x, see Table 3.9.

Table 3.9: Ammonia injection inlet data.

Inlet data		Units
Temperature	20.0	°C
$NH_3/NO_{initial}$	1.30	
NH_3	0.0167	kg/s
NH_3 in water	10.5	mol%
H_2O	0.151	kg/s

Figure 3.9 illustrates the selective non-catalytic reduction (SNCR) process occurring in the model when inserting the mix of ammonia and water into the recovery boiler. The ammonia mix is inserted in between the quaternary air in the combustion section, Figure 3.7, and the steam generation, Figure 3.8, due to the narrow temperature interval described in Section 2.3.2. The stoichiometric reactor (SNCR) in the model will represent the SNCR reaction, Equation 2.23, happening in the boiler.

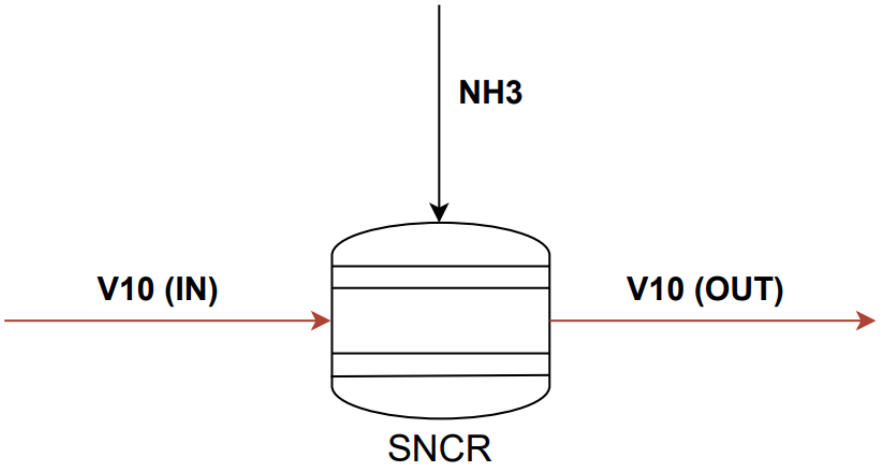

Figure 3.9: Model integration of the ammonia injection.

By implementing the water-diluted ammonia injection into the model for NO_x reduction as an SNCR method, the effects on the operational conditions of the boiler were examined and are presented in the results.

Södra was also interested in investigating the possibilities of injecting the so-called 'dissolver off gas' into the boiler. The idea was that the ammonia-containing gas could possibly provide an SNCR-type effect for NO_x reduction when fired into the boiler, at a similar injection point as the water-diluted ammonia injection. Earlier studies done by ÅF at several Swedish mills had shown no increase in NO_x emissions for this type of gas firing, but there was also no evidence of an SNCR-effect. As described in Section 2.2.3, the cyanate formed in the green liquor is partly converted to NH_3 when entering the dissolver tank. Ammonia is then removed from the dissolver by two identical fans by adding a flow of air.

The nitrogen content in the smelt was not measured on site, therefore, the NH_3 formed from the green liquor was approximated based on the assumption that half of the cyanate in the green liquor formed NH_3 in the dissolver tank. Such high conversion rates in the dissolver were uncommon based on the study by ÅF [24]. Through this approximation, an upper bound of the NH_3 availability from the dissolver off gas on site was set.

Some of the dissolving off gas inlet data collected from Södra is shown in Table 3.10. Calculated flows of NH_3 in the dissolving off gas and the NH_3 concentration in the flue gas when injecting the gas are presented in Appendix B.1.

Table 3.10: Dissolver off gas inlet data [20].

Inlet data		Units
Temperature	341	°C
Total mass flow	13.3	kg/s
Air flow	11.3	kg/s
H_2O in air	2.03	kg/s

After calculating the approximated amount of NH_3 in the dissolver off gas, a similar implementation to the water-diluted ammonia injection was performed for the gas injection in the model, and the operational conditions of the boiler were compared between the two methods. The dissolver off gas was injected into the COMB2 at the quaternary air level, where the exhaust gas temperature is at its lowest before entering the steam generation region. Two different cases were simulated for this injection.

In Case 1, the dissolver off gas was simply added together with the initial airflow of quaternary air. For Case 2, the quaternary air flow was decreased and exchanged with the dissolver off gas, since this gas mainly consists of air. Ultimately, results for the flue gas composition, temperature, and heat load between the two cases were compared.

3.4.2 Recycling of scrubber effluent

In a parallel study, the design of a scrubber for wet flue gas treatment of NO_x and SO_x was performed, also as a case study for Södra's process. This technique is explained in Section 2.4, where the idea of recycling the scrubber effluent back to the recovery boiler was investigated as a primary measure.

For the wet flue gas treatment study, the scrubber was modeled in Aspen Plus using a thermodynamic model called ELEC-NRTL, which is applicable for aqueous and mixed solvents. The effluent stream, therefore, contained ionic compounds that had to be converted into uncharged compounds compatible with the recovery boiler model. See Appendix B.2 for calculations. These compounds are compiled in Table 3.11, followed by the corresponding volumetric flow and temperature of the stream.

Table 3.11: Inlet effluent stream data.

Effluent		Units
N_2	9.5	g/s
CO_2	22	g/s
Na_2SO_4	0.17	kg/s
H_2O	1.2	kg/s
Total flow	4.6	m^3/h
Temperature	58	℃

The effluent inlet data was inserted at the secondary air level into the model by adding a stream, and relevant changes in the mass and energy balances compared to the base case were observed. Since the Aspen model was limited in simulating dust formation in the boiler, the sulphidity in the flue gas as well as the sulphur and sodium losses to the stack were calculated in Excel for the modified case, similar to Appendix A, Table A.7.

To simplify the addition of sodium and sulphur to the system in Excel, the share of recycled dust remained the same, based on the total amount of sodium entering the boiler. In order to approximate the amount of gaseous sulphur in the flue gas, the increase of SO_x and TRS was assumed to be linear in the flue gas when adding the effluent.

4

Results

In this chapter, the results from the Aspen simulations are presented, along with the mass and energy balances, to provide an understanding of the model's performance, sensitivity, constraints, and key findings. First, the model is validated by comparing data from both literature and Södra. This is followed by a sensitivity analysis of the air staging. Subsequently, the results from the different primary measures are also displayed.

4.1 Model validation

4.1.1 Mass and energy balances

The following tables present the most important data for comparison between the simulated results from the base case and the literature-based mass and energy balances, along with some of the reference data collected from Södra. Table 4.1 shows the smelt composition of the inorganic compounds as well as the desired reduction efficiency.

Table 4.1: Smelt composition, flow and reduction efficiency compared to the literature.

Variable	Simulation	Literature	Units
Na_2S	23.0	22.4	wt%
Na_2CO_3	66.2	67.0	wt%
Na_2SO_4	2.68	2.60	wt%
NaCl	0.562	0.562	wt%
K_2CO_3	7.54	7.52	wt%
Mass flow smelt	23.5	23.6	kg/s
Reduction efficiency	94.0	94.0	%

In Table 4.2, the simulated air flows are presented and compared with the flows from mass balance calculations from the literature. The primary air represents the required air supply to reach the desired reduction efficiency in the lower part of the furnace. It can be seen that the simulated primary air is half the amount compared to the reference data, but that the amount of secondary air compensates for this to achieve similar total amount of air supply.

Table 4.2: Air inlet flows compared to the literature and collected inlet data from the design specifications.

Variable [Nm^3/s]	Simulation	Literature	Inlet data
Primary air	24.95	26.79	47.71
Secondary air	82.57	-	59.81
Teriary air	11.01	-	11.01
Quaternary air	31.98	-	31.98
DNCG	11.90	-	11.90
Total air supply	162.4	163.8	162.4

Table 4.3 presents the simulated composition and total flow of the flue gas. These values are compared with calculated literature data, alongside reference data obtained from the DGE and ILEMA measurements. The compositions, presented in volume percentages, were calculated based on a wet gas basis. The fractions of NO_x and SO_x presented in the table are referred to as NO_2 and SO_2 respectively.

Table 4.3: Flue gas composition and flow compared to the literature, DGE's and ILEMA's measurement as reference data.

Variable	Simulation	Literature	DGE	ILEMA	Units
O_2	2.76	2.82	3.10	2.45	vol%
H_2O	20.7	20.5	18.4	20.9	vol%
CO_2	12.8	12.7	10.3	12.7	vol%
N_2	63.7	63.9	-	-	vol%
NO_x	62.4	-	70.0	-	ppmv
SO_x	< 1.00	-	< 1.00	-	ppmv
CO	376	-	100 - 500	150-550	ppmv
HCl	< 1.00	-	< 2.50	-	ppmv
Total flow	201.8	203.8	241.7	220.1	Nm^3/s
Total flow dry	161.0	160.3	197.3	173.9	Nm^3/s

In validating the temperature distribution in the boiler, the the reported design specifications served as the primary reference for matching the heat transfer to the tube walls and obtaining the desired steam and flue gas temperatures, as shown in Table 4.4.

Table 4.4: Regional temperatures in comparison to reference data from the design specifications.

Variable [°C]	Simulation	Ref. data
Smelt	1003	900-1100
Between primary and secondary	1726	1596
Between secondary and tertiary	1460	1455
Above tertiary	1304	1301
Above quaternary	1101	1084
Flue gas temp	195.1	195.0
Steam temp	480.0	480.0

Table 4.5 shows the simulated heat exchanger loads required to achieve the desired steam production while maintaining temperatures in the range of the design specification temperatures. To clarify, the excess heat load represents the additional heat that was removed to reach an exhaust temperature of 195 °C for the simulation.

Table 4.5: Heat exchanger units and excess heat load in flue gas.

Variable [MW]	Simulation
Heat load to walls	208
Superheater & Economiser	300
Heat load to steam	505
Excess heat load	51.9

In Table 4.6, the overall heat load input to the boiler, losses and heat load to steam are presented and compared with the energy balance from the literature and the reference data from Södra. The total heat load covers not only the radiation and unaccountable losses but also the heat for formation of Na_2S in the smelt, the sensible heat in the flue gas in the stack and in the smelt leaving the boiler. See Appendix A, Table A.8.

Table 4.6: Overall energy balance compared to the literature and reference data.

Variable [MW]	Simulation	Literature	Ref. data
Heat load to steam	505	496	460
Total heat load losses	-	170	177
Total heat load input	-	666	637

4.1.2 Sensitivity analysis

In this section, the results from the sensitivity analysis for investigating the performance and stability of the model are presented.

Considering the performance of the boiler at the lower region, reduction efficiency serves as a critical indicator in particular. Therefore, Figure 4.1 presents a sensitivity analysis of primary and secondary air, given their importance in black liquor combustion.

As shown in Figure 4.1 each curve corresponds to a fixed secondary air flow. Variation in primary air flow yields new operating conditions and their respective reduction efficiencies. Despite varying secondary air, all cases show a similar trend, where reduction efficiency inversely correlates with primary air flow. Altering the secondary air did not impact the reduction efficiency significantly, as can be seen in the figure.

For a fixed primary air flow of 24.95 Nm^3/s, all cases demonstrate a reduction efficiency of 94 % or higher. The green line represents the secondary air supply from the base case of 82.57 Nm^3/s.

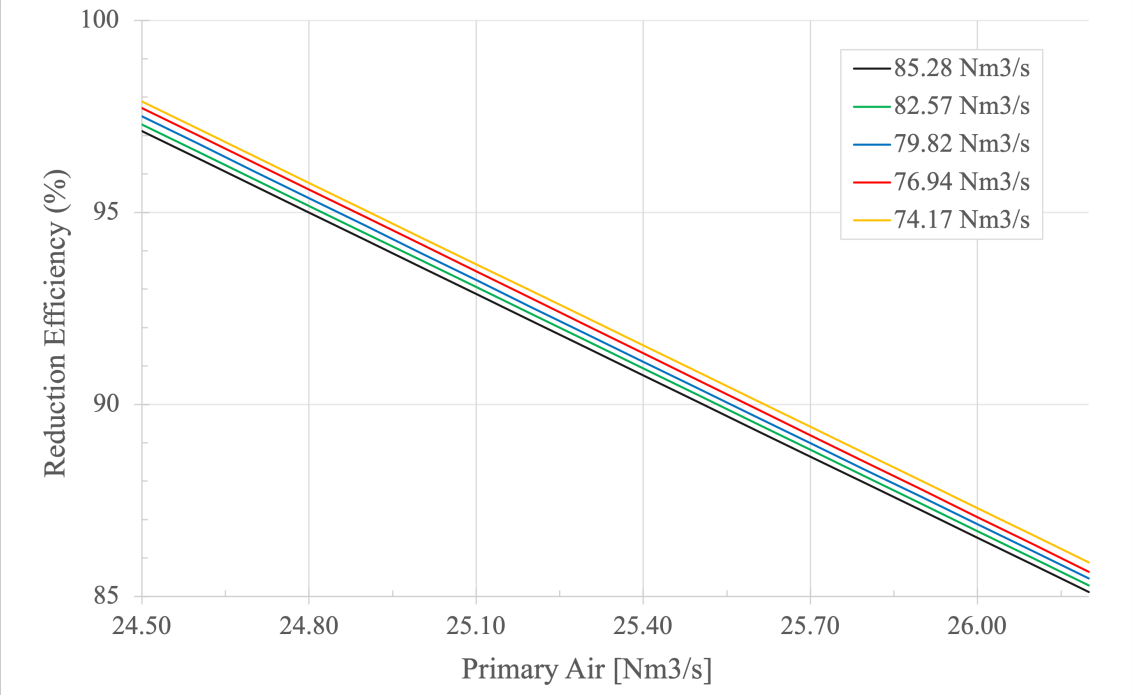

Figure 4.1: Reduction efficiency in relation to primary air, for different secondary air flows.

Figure 4.2 is similar to the figure above as it depicts the relationship between reduction efficiency and primary air. However, it also demonstrate the relation in the flue gas temperature. It is shown that as the primary air is increased, the reduction efficiency decreases while the flue gas temperature rises.

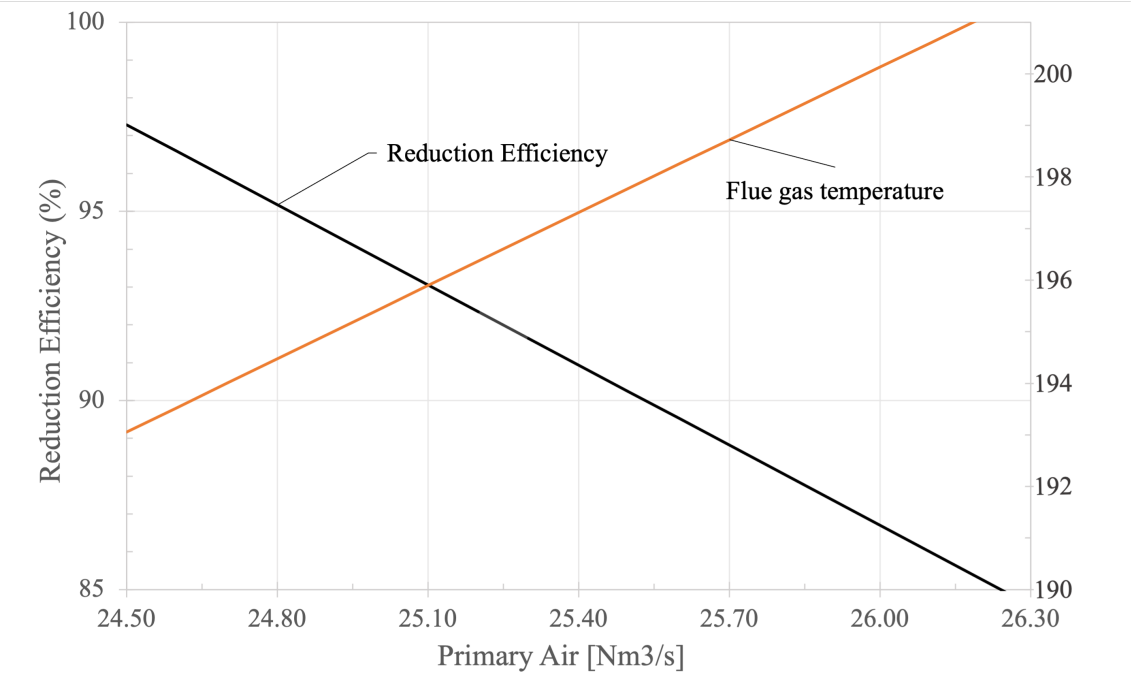

Figure 4.2: Flue gas temperature and reduction efficiency in relation to primary air flow (secondary air same as base case: 82.57 Nm^3/s).

Considering the evaluation of performance for the upper part of the furnace in the model, Figure 4.3 illustrates how the overall composition of the flue gas is affected by increased temperatures at nose level, after the quaternary air injection. The differential increase or decrease in vol% for each component is shown in the figure, based on the initial flue gas composition at 1100 °C.

It can be seen that for a temperature increase to 1600 °C, which was needed to reach a CO level of 376 ppmv in the flue gas for the model, the O_2, N_2, and H_2O content changed by less than 0.02 vol%. The CO_2 content decreased less than 0.04 vol% at this temperature increase. Furthermore, the overall flue gas composition at this CO level corresponds to the composition in Table 4.3.

Another notice is that the change in composition exhibits an exponential trend with increased flue gas temperature.

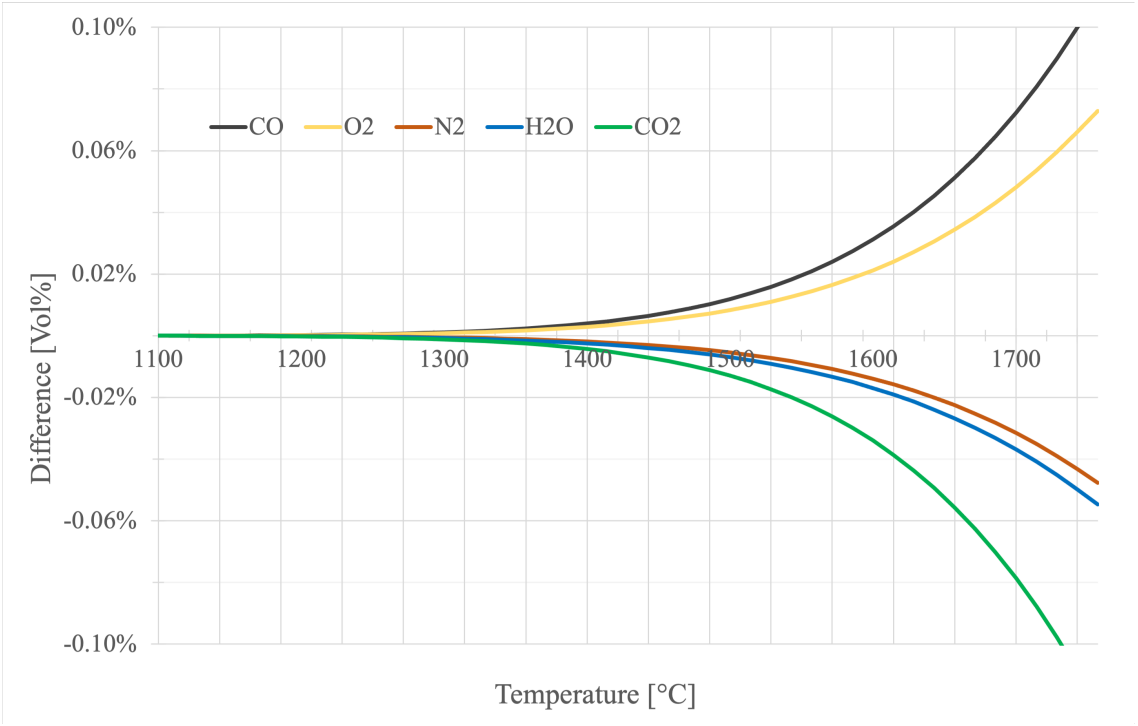

Figure 4.3: Deviations in the flue gas composition, starting from 1100°C, with increased temperature, above quaternary air level.

The same increase in CO content (376 ppmv) in the flue gas can be observed in Figure 4.4 as the temperature at nose level rises in the model. The CO content is less than 1 ppmv at the initial temperature of 1100 °C.

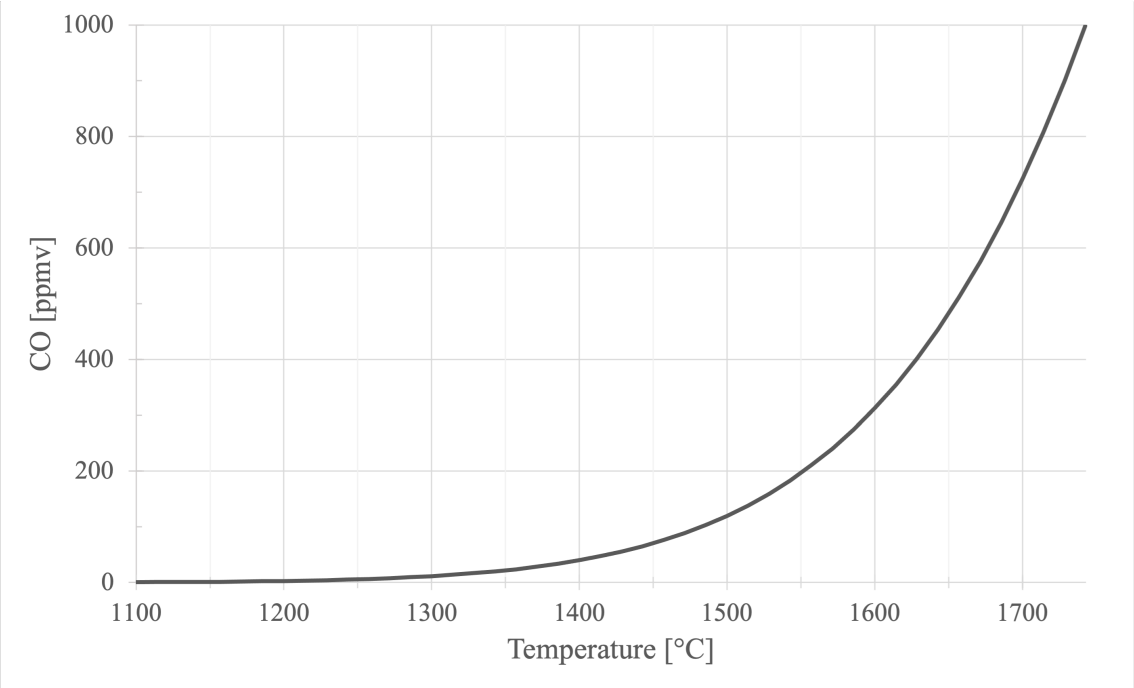

Figure 4.4: CO level in flue gas with increased temperature, above quaternary air level.

4.2 Primary measures

4.2.1 Ammonia injection

Results from the water-diluted ammonia injection to the boiler is shown in Table 4.7, where the reduction of NO_x emission was set to 45 % at full operating load. The table provides data on the quantities of NH_3 injected, initial NO, and resulting NO after reduction. It also shows the provided heat load loss in the flue gas when injecting from the simulation. The unit mg/Nm^3 is per dry flue gas at reference 6 % O_2. The change in flue gas composition was negligible due to the small amount injected. However, the flue gas temperature decreased with 1 °C.

Table 4.7: NO_x reduction and flue gas heat load losses with water-diluted ammonia injection.

$NH_3/NO_{initial}$	NH_3 mol/s	NH_3 mg/Nm^3	$NO_{initial}$ mol/s	NO_{final} mol/s	Losses MW
1.3	0.98	74	0.76	0.42	2.5

Comparing the NO_x reduction with the yearly specific emission values from the BAT requirements, the values of $NO_{initial}$ and NO_{final} from Table 4.7 were converted to mg/Nm^3 at 6 % O_2 per dry flue gas, as shown in Table 4.8. In the table, 'Södra' refers to their Environmental Report from 2023.

Table 4.8: Initial concentrations of NO_x from different reference data and final concentration of NO in dry flue gas, with water-diluted ammonia injection.

Concentration of NO	Södra	DGE	BAT	NO_{final}
mg/Nm^3	141	100	120 - 250	55.0

The optimal concentration of ammonia may differ depending on the recovery boiler operating conditions. Therefore, Figure 4.5 illustrates the relationship between ammonia concentration (water-diluted) and heat load loss. The amount of NH_3 is fixed while the amount of water is varied. It can be observed that a lower concentration of ammonia results in a larger loss in heat load, by an exponential increase. Achieving a balance between the concentration of ammonia and the reduction of NO_x emissions can, therefore, be a factor to consider.

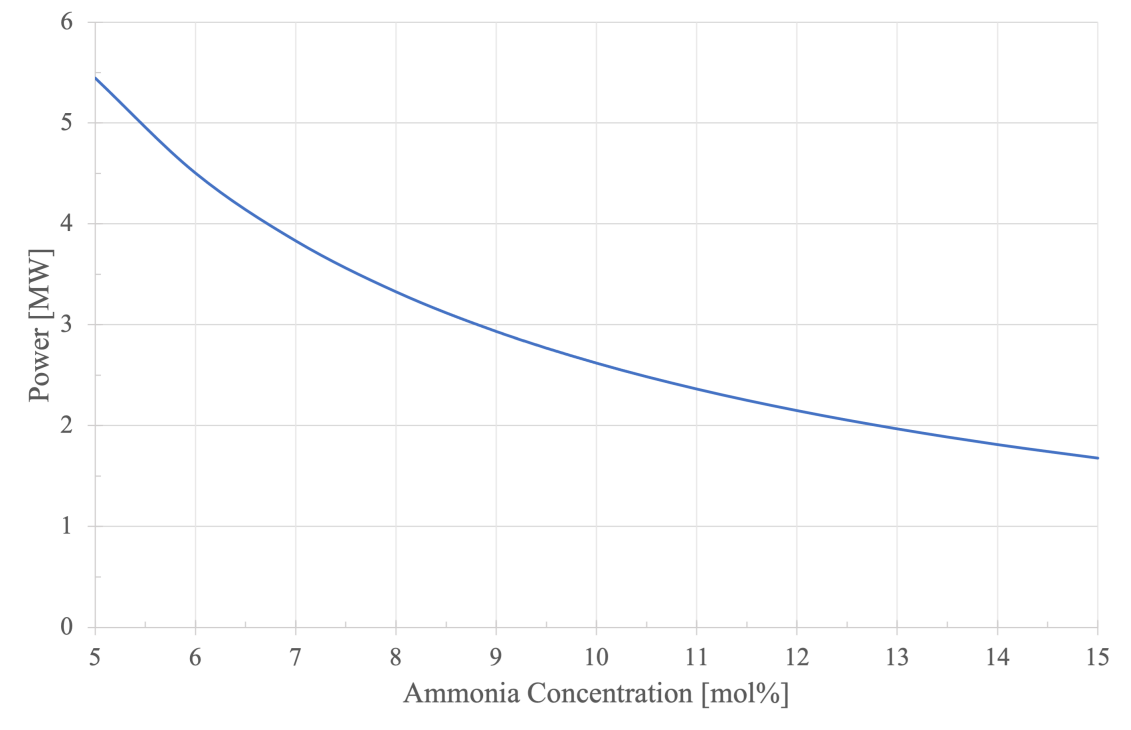

Figure 4.5: Ammonia concentration in relation to heat load loss.

Results from the dissolver off gas injection are shown in Table 4.9 and 4.10. Table 4.9 provides a comparison of the calculated ammonia dosages in mg/Nm^3 at 6 % O_2 per dry flue gas with the addition of dissolver off gas (Case 1) and decreased flow of the quaternary air (Case 2).

Table 4.9: Ammonia dosage in flue gas comparison with adding dissolver off gas (Case 1) and decreased flow of 4^{th} air (Case 2).

Dissolver off gas	Base Case	Case 1	Case 2	Units
$NH_3/NO_{initial}$	-	0.389	0.389	
NH_3	-	0.294	0.294	mol/s
NH_3	-	20.9	22.1	mg/Nm^3
Dis. off gas flow	-	11.3	11.3	Nm^3/s
Quaternary air flow	32.0	32.0	20.7	Nm^3/s

In addition, Table 4.10 compares the composition, temperatures, and heat load increase in the flue gas based on model simulations, with the same cases as the table above. The vol% is based on wet flue gas.

Table 4.10: Comparison of composition, temperatures and heat load increase in flue gas with added dissolver off gas (Case 1) and decreased flow of 4^{th} air (Case 2).

Dissolver off gas	Base Case	Case 1	Case 2	Units
O_2	2.76	3.45	2.47	vol%
H_2O	20.7	20.8	21.9	vol%
CO_2	12.8	12.2	12.8	vol%
N_2	63.7	63.6	62.7	vol%
Temperature	195	205	211	°C
Increased heat load	0	22.4	22.5	MW

Comparing the ammonia availability in the water-diluted ammonia and the dissolver off gas inlet(Table 4.7 and Table 4.9), the molar flow difference was 0.69 mol/s.

4.2.2 Scrubber effluent recycling

Results for the scrubber effluent recycling were provided by the calculations on sulphur and sodium balances from the base case compared to the case when the effluent entered the boiler. As shown in Table 4.11, the S/Na_2 ratio increases in the black liquor but decreases in the flue gas inside the boiler. Additionally, the loss of sulphur and sodium to stack was decreased. Overall, the comparison shows no drastic changes to the sodium and sulphur balance when the effluent was injected.

Table 4.11: Sulphur and sodium balance from base case compared to the case with recycled scrubber effluent.

	Base case	Recycled effluent	Units
Total S to boiler	2.37	2.40	kg/s
Total Na to boiler	10.2	10.3	kg/s
S/Na_2 in black liquor	0.324	0.327	mol/mol
Total S in flue gas	0.608	0.611	kg/s
Total Na in flue gas	1.02	1.03	kg/s
S/Na_2 in flue gas	0.858	0.856	mol/mol
S loss to stack	0.274	0.269	wt%
Na loss to stack	0.106	0.106	wt%

Table 4.12 presents how the flue gas composition and temperature are affected when inserting the scrubber effluent in Aspen, as well as the reduction efficiency and heat load loss. The reduction efficiency of the smelt increased with the same amount of total air flow as in the base case, and the temperature in the lower region of the boiler did not increase significantly. On the other hand, the flue gas temperature decreased by 7 °C, resulting in a corresponding heat load loss.

Table 4.12: Flue gas composition, heat load loss and reduction efficiency from base case compared to the case with recycled scrubber effluent.

	Base case	Recycled effluent	Units
O_2	2.76	2.69	vol%
H_2O	20.7	21.3	vol%
CO_2	12.8	12.8	vol%
N_2	63.7	63.2	vol%
Reduction efficiency	94.0	94.6	%
Flue gas temperature	195	188	°C
Heat load loss	-	20.5	MW

5

Discussion

According to the literature study of this thesis, the applications for primary measures on kraft recovery boilers are numerous. There are still many of uncertainties among the newly implemented technologies that have not been tested or understood due to the chemical complexity in the boiler. Collecting relevant data at Södra made it possible to investigate possibilities for emission control and how these implementations affected the process as a whole. Based on the results, both ammonia injection and recycling of scrubber effluent have the potential for emission control as primary measure technologies. However, more research is needed in the future before an implementation is possible.

5.1 Model validation and limitations

Validating the Aspen model, followed by a sensitivity analysis, was a crucial part of the work to ensure the reliability of the primary measures being investigated. The validation showed good predictability in general, compared with the theoretical mass and energy balances from the literature. However, the biggest uncertainties relied mainly on the air and temperature distribution in the model. Although the inlet temperatures and the total air flow were close to reality, the zero-dimensional model did not account for the spatial behaviour of the species in the boiler. Each reactor operated under perfectly mixed conditions aimed at achieving equilibrium, introducing uncertainties regarding the final flue gas composition and temperatures in each region of the boiler.

5.1.1 Smelt and reduction efficiency

The validation of the smelt composition in Aspen with values from Södra was not possible since measurements of the whole composition could not be obtained from inside the boiler. Södra only measured Na_2S, Na_2CO_3, and Na_2SO_4, which did not provide a representative comparison. However, the reduction efficiency was given which was used to steer the main compounds in the smelt according to Equation 2.13. Comparing the compositions in the smelt showed similar results with small errors between the simulation and the literature, see Table 4.1.

However, one limitation of the model is that it did not consider the formation of dust from Na, S, Cl, and K compounds in the smelt. The smelt composition obtained from the simulation could, therefore, deviate compared to reality. Although results from the mass balances in Excel only indicated small losses of sodium and sulphur, both to the flue gas and further to the stack. This could also be explained by the fact that a smelt temperature of approximately 1000 °C should minimise the vaporisation of both sulphur and sodium, as explained in Section 2.2.1. The small losses should, therefore, not effect the smelt composition significantly.

5.1.2 Air flows

The validation of the air flows in the model showed similar results in total. However, achieving the same primary air flow as in Södra's case was not possible. Table 4.2 demonstrates that the Aspen model could only handle approximately half (48 %) of the primary air compared to Södra. However, when comparing with the literature, the error is only approximately 7 %. This may be explained by the fact that Aspen only requires the amount of primary air needed to reach a certain reduction efficiency in a reactor with perfect mixing and equilibrium-based reactions. In reality, the air supply needs to be much higher since the compounds in the char bed have a more limited reaction surface. To achieve the same total air supply as Södra and ensure the correct mass balance in the model, the missing amount of primary air was inserted into the secondary air flow instead.

Subsequently, when performing the sensitivity analysis on the primary and secondary air in relation to the reduction efficiencies, stable and predictable results were obtained, see Figure 4.1. This stability can be attributed to the reduction efficiency's reflection of its ability to recover inorganic compounds from white liquor, to maximise this efficiency. Furthermore, all cases demonstrate a similar trend, where reduction efficiency inversely correlates with primary air flow, despite variations in secondary air. Ensuring a reducing atmosphere requires a precise primary air supply to balance O_2 consumption by carbon and Na_2SO_4 reduction, thus promoting a high formation of Na_2S. In the model, only a small fraction of the supplied secondary air was distributed to the reduction zone which can explain why its influence on the reduction efficiency was insignificant. While the secondary air influences carbon distribution and may potentially convert it to gaseous oxides before reaching the char bed's active layer, Figure 4.1 confirms that this is not significant in impacting reduction efficiency.

Another observation is that increasing the primary air supply decreases the reduction efficiency in the smelt, while the flue gas temperature rises, see Figure 4.2. Based on these results from the model, it can be concluded that the reduction efficiency can be regulated by adjusting the available oxygen provided by the primary air. However, there will be a trade-off between increased flue gas temperature, leading to higher steam generation, and lower reduction efficiency, and vice versa.

5.1.3 Flue gas flow and composition

Overall, the validation of the model yielded promising results when comparing the main components and flow of the flue gas between the simulation and literature values. One rather surprising finding from the validation was that the total flue gas flow measured by DGE was significantly higher compared to the simulation results, see Table 4.3. One possible explanation for this discrepancy could be the challenges associated with accurately measuring flue gas flow, as noted in both the DGE and ILEMA reports. Additionally, the start burners used for startup were not included in the Aspen model, which could also contribute to the error between the simulation and DGE. The lower H_2O content in the flue gas measured by DGE can likely be explained by the fact that the black liquor contained less water upon entering the boiler during the measurement. The DGE measurements differed more from the simulated values than the ILEMA measurements. Although the DGE report was considered more reliable as reference data since the measurements were more up-to-date with the current boiler setup compared to the ILEMA measurements from 2019.

As outlined in Section 3.2.2, the model maintained CO levels in the flue gas below 1 ppmv, achieved through complete mixing and full combustion. When exploring the impact of temperature on CO levels (Figure 4.4) it became evident that the formation of CO is closely correlated to temperature in the model. Fortunately, when matching the CO level with industrial data, increasing the temperature did not significantly affect the results or validation of the main components in the flue gas (see Figure 4.3).

However, the achieved CO value of 376 ppmv represents an average derived from measurements conducted by both DGE and ILEMA. The actual CO levels exhibit frequent fluctuations, ranging between 100-1000 ppmv during the measurements. In Södra's case, elevated CO levels do not stem from temperatures reaching 1600 °C above the quaternary air, rather, they result from hot or cold spots and inefficient combustion within the recovery boiler. Possible causes include inadequate or uneven air distribution, leading to improper mixing. In a well-operated recovery boiler, CO levels in the flue gas typically remain below 100 ppmv. Ideally, CO levels should be even lower, around 10-50 ppm, to indicate complete combustion. Although achieving a more efficient combustion could potentially lead to higher NO_x levels, presenting a trade-off, further investigation into optimising combustion efficiency in the boiler could, therefore, be interesting.

5.1.3.1 Formation of NO_x and SO_x

The formation of NO_x in the recovery boiler heavily relies on kinetics-based reactions. However, Aspen cannot accommodate these complex reactions, undermining the credibility of NO_x formation predictions. Additionally, the simulation did not consider the size distribution of the black liquor droplets entering the boiler, further introducing uncertainties in the black liquor devalorisation. As discussed in the theory, see Section 2.3.1, the size of black liquor droplets impacts the distribution of fuel nitrogen between the smelt and flue gases as N_2 or NO_x, a factor that could not be evaluated through model simulations.

In order to achieve the same level of NO_x emissions in the model as Södra has, N_2 was made inert in the reactors to exclude the formation of NO_x that required integration with N_2 from the air. Consequently, only NO_x derived from the nitrogen in the black liquor was accounted for, resulting in 62.4 ppmv of NO_x in the flue gas.

Unfortunately, it was still not possible to investigate the formation routes of black liquor nitrogen in the flue gas. The formation of NH_3 from the devalorisation of the black liquor, followed by its oxidation to NO, was not observed in Aspen (see Section 2.7). Additionally, the conversion to char nitrogen could not be tracked. However, according to the theory, both prompt NO_x and thermal NO_x are considered quite small compared to fuel NO_x. Therefore, the amount of NO_x formed from black liquor nitrogen can be conserved to achieve the correct mass balance in the model.

Following the reasoning above, accurately modelling the formation of NO_x was not feasible due to its high complexity. As a result, implementing primary measures in the model does not provide direct conclusions regarding the increase or decrease of NO_x. Instead, insights can be drawn from earlier studies, theoretical analysis, and the results of the mass and energy balances.

Since Södra already has very low SO_x emissions, this aspect was not investigated as thoroughly. The primary focus was on analysing the sulphur balance and sulphidity within the boiler.

5.1.4 Temperature and energy

The temperature and steam generation results indicated promising reliability for the model, as seen in Table 4.4 and 4.6. This was somewhat expected since the temperatures in the different regions were adjusted to align with reference temperatures from the reported design specifications. Heat was exchanged from the volatiles to the tube walls throughout the boiler, resulting in a steam temperature of 480 °C. However, the temperature region between the primary and secondary air levels did not align as well as the other regions. Given the lack of spatial temperature distribution in the Aspen model compared to the more reliable design specification, it was anticipated that not all temperature regions in the boiler would fully match.

From the simulations, the excess heat load of 51.9 MW likely corresponds to unaccountable losses and radiation losses, which Aspen does not consider. This excess heat load should not be confused with the total heat loss presented in Table 4.6. The latter also includes the useful energy for sensible heat in the smelt and flue gas exiting the boiler, as well as the heat required for the formation of Na_2S in the smelt.

The 'heat load to steam' presented in Table 4.6 was lower for the reference data compared to the simulation. However, Södra also reports their heat loads based on calculated values, which may not be consistent with the calculation method through this thesis. This variability increases the uncertainty when comparing the heat load from this work with Södra's data and makes it challenging to draw direct conclusions about why these values differ.

5.2 Primary measures

5.2.1 Ammonia injection and dissolver off gas

When evaluating both the ammonia injection and dissolver off gas, Aspen was used solely to investigate the difference in heat load since it cannot simulate NO_x formation, nor the ammonia slip. Therefore, when evaluating water-diluted ammonia injection in the model, experimental data from the study by Metso Power was used, presented in Table 4.7. The results showed that reducing NO_x emissions by 45 % resulted in an energy loss of only 2.5 MW from the simulation, which is reasonable given the large flue gas flow compared to the relatively small amount of water injected. Additionally, Figure 4.5 shows how the flue gas heat load loss increases exponentially with a lower ammonia concentration, since more added water cools the boiler.

By comparing the yearly emission concentrations from the reference data with the NO_x reduction (see Table 4.8), the NO_x emissions are reduced below the limit. Due to the promising results from water-diluted ammonia injection in many experimental tests, further investigation is suggested. However, there are several uncertainties regarding NO_x reduction, such as the narrow temperature interval in which ammonia injection is effective, finding the optimal concentration, and other factors. This SNCR method will be discussed further in Section 7.

Another interesting measure to investigate, though not as thoroughly tested, is the use of dissolver off gas, which is already available on site at Södra. The Åbo study described in Section 3.9 showed no significant results for NO_x reduction when recirculating the dissolver off gas into the boiler. However, the low amount of ammonia in the dissolver off gas could explain the lack of observed reduction.

Two cases were investigated compared to the base case. Table 4.10 shows the comparison between composition, temperature, and the increased heat load when incorporating these cases into the model. The composition in Case 1 changes because the process involves adding dissolver off gas without reducing other air flows, leading to a dilution effect rather than a significant shift in the gas balance. In Case 2, it was observed that the concentrations of O_2 and N_2 decreased since the pure air was replaced with dissolver off gas containing other compounds, such as NH_3 and more H_2O, thereby also increasing the level of H_2O.

Additionally, one could argue that in Case 1 the increased levels of O_2 concentration and the rise in temperature could both lead to increased emissions of NO_x, as these conditions are typically favourable for thermal NO_x formation. Furthermore, elevated O_2 levels and temperatures typically result in more efficient combustion thereby reducing CO levels as CO can be oxidised to CO_2. On the other hand, Case 2 demonstrates a decrease in O_2 levels indicating a limited availability of O_2 to form NO_x. It is uncertain whether the CO levels would increase or decrease in this scenario, considering the higher combustion temperature favouring the reduction, but the lower excess of O_2 does not.

The difference in ammonia presented in the results (0.69 mol/s) may indicate that an additional amount of ammonia is required to achieve a similar reduction. However, determining whether the reduction rate of dissolver off gas matches that of water-diluted ammonia when injecting the same amount of NH_3 is challenging due to the different mixing behaviour of NH_3 in the air compared to water. This aspect will be further explored in Section 7. Another drawback of this could be the potential increase in oxidation of NH_3 to NO_x when injected at such high inlet temperatures (341 °C). The rise in flue gas temperature is evident in Table 4.10. Thus, optimal placement for injection into the boiler becomes even more critical in this scenario.

It could be advantageous for the company to utilise the dissolver off gas stream as a SNCR method, as the waste stream and consequently the NH_3 can be recycled. Successfully implementing the gas for NO_x reduction would eliminate the need for additional NH_3 and quaternary air to some extent, and could thereby reduce costs and potentially mitigate future NO_x fees.

5.2.2 Scrubber effluent recycling

The S/Na_2 ratio for both the flue gas and the black liquor remained relatively unchanged upon the addition of the effluent stream. This is because the contribution of sodium and sulphur from the effluent was much smaller compared to the total sodium and sulphur content from the black liquor entering the boiler, as shown in Table 4.11. Although the losses of sulphur and sodium to the stack decreased slightly, the overall impact on the S/Na_2 ratio was not significant. Additionally, the similarity in the S/Na_2 ratio can be explained by the fact that the effluent stream, containing Na_2SO_4, maintains a molar equivalence between sodium and sulphur, thereby preserving this ratio.

On the other hand, injecting additional sodium and sulphur into the boiler would supposedly decrease the requirement for make-up chemicals. Considering the increase in reduction efficiency observed in the simulation results (Table 4.12), where the air flows remain the same as in the base case, there is a possibility of reducing the need for make-up Na_2SO_4 to form Na_2S while still achieving a reduction efficiency of 94 %. However, further investigation is necessary to determine whether the effluent compounds behave similarly to the make-up chemicals in the boiler. Achieving a higher reduction efficiency also allows for a higher flow of primary air that could decrease the efficiency back to 94 %. This could in turn improve the combustion efficiency and decrease CO levels, as more excess oxygen is available.

Considering the change in flue gas composition when injecting the effluent, Table 4.12 shows that the H_2O content increased while the O_2 and N_2 decreased, indicating that the injection of water dilutes the flue gas. The share of CO_2 remained unchanged, likely due to both the CO_2 amount from the effluent and the dilution effect on the flue gas.

It was only possible to make assumptions about how the rate of vaporisation of S and Na from the lower part of the furnace would change. However, since there was no significant increase in temperature in this region when adding the effluent, one could conclude that the formation of sodium and sulphur compounds in the dust is similar to the base case. Whether more TRS or SO_x is formed by adding the effluent stream remains uncertain, but it can be argued that the increase in total gaseous sulphur is similar to that of the base case.

For instance, if a higher amount of effluent were injected, it is likely that the sulphidity in the flue gas would increase due to the temperature decrease in the smelt, releasing more gaseous sulphur and less sodium, as explained in Section 2.2.1. According to Section 2.2.2, one could also argue that the S/Cl ratio in the flue gas would increase, resulting in more formation of HCl compared to NaCl in the dust. A lesser amount of NaCl formed in the flue gas would then decrease the fouling and corrosive tendency in the boiler. However, the effects on sulphur oxides formation routes are rather complex, making it challenging to draw any evident conclusions.

Adding more effluent into the boiler would, on the other hand, cool the boiler, as more water is injected, reducing the useful heat for producing steam in the flue gas. However, an interesting scenario would involve evaporating the water from the effluent stream before injecting it into the boiler, thereby minimising the impact of water on the boiler's performance.

Due to limitations in Aspen, no clear results regarding the effects on NO_x reduction were attainable with this implementation. Therefore, further investigation is necessary, especially considering that NO_x reduction has been successfully achieved in previous experiments (see Section 2.4). The environmental benefits for the company could be substantial, as having both an efficient scrubber to reduce NO_x and recycling the waste stream back to the boiler for further reduction. This approach also reduces the amount of effluent that needs to pass through the wastewater treatment facility and prevents some release of NO_x into the atmosphere from this process.

When considering all three emission control technologies discussed in this section, it is important to consider the risks of injecting water into the boiler. As described in section 2.3.2, injecting water into the boiler could potentially cause an explosion. If the water comes into contact with the smelt, the rapid conversion of water to steam will create very large volumes, or it may decompose into hydrogen and oxygen, which can then ignite. The amount of water in all three streams is equal to or less than 2 kg/s. Given the relatively small amounts, it is unlikely that an explosion would occur as the water would evaporate before reaching the smelt. However, further investigation is required to ensure this, or whether it is possible to evaporate the water before it enters the boiler, as described above.

6

Conclusion

As a case study of Södra Cell Mönsterås's recovery boiler, this thesis evaluate the primary emission control measures for the kraft pulp mill process. The use of Aspen Plus allowed for detailed modelling of the boiler's mass and energy balances and was successfully validated. However, further refinement is needed, particularly for the spatial distribution of air and temperature within the boiler. The zero-dimensional and equilibrium-based nature of the model introduced some limitations, mainly in handling the kinetic-based reactions necessary for predicting NO_x formation. Therefore, conclusions regarding NO_x formation were limited and based on theoretical and literature findings.

The effect on the mass balances in the model for water-diluted ammonia injection showed no change in the flue gas composition and for the energy balance it showed a minimal heat load loss of 2.5 MW.

For the dissolver off gas in Case 1, the CO level in the flue gas may be reduced due to the higher excess of O_2 and the increased flue gas temperature. However, this could also result in increased formation of NO_x. In contrast, the decreased excess of O_2 in Case 2 could thereby limit the formation of NOx. Moreover, the current amount of NH_3 from the dissolver off gas may be insufficient to achieve any significant effects for SNCR in the boiler.

The dissolver off gas injection increased the flue gas temperature in both cases, thereby increased the steam generation. However, the high inlet temperature of the gas may worsen the reduction of NO_x. From an economical and environmental point of view, this implementation would be preferable considering the utilisation of a waste stream.

The injection of scrubber effluent into the boiler did not significantly alter the S/Na_2 ratio in the flue gas or black liquor, and no evidence for increased formation of SO_x was determined. Additionally, simulation results showed an increase in reduction efficiency (94.6 %) without altering the air flows, suggesting a decreased need for make-up chemicals (Na_2SO_4). However, increasing the required primary air flow needed for reaching the same reduction efficiency (94 %) could potentially decrease the formation of CO but instead increase the NO_x formation due to the excess of oxygen in this region. Combining efficient scrubber technology with effluent recycling could provide significant environmental benefits, reducing the load on wastewater treatment while mitigating NO_x emissions.

7

Future work

To be able to understand and evaluate the issues addressed in this thesis, it would be beneficial to further develop a more detailed boiler design capable of accurately simulating kinetic-based reactions, such as the formation of NO_x. Additionally, further investigation into aspects such as the spatial distribution of air and temperature, as well as the size distribution of black liquor droplets would be valuable. Improving the model would supposedly be the first step. Subsequently, conducting experiments for implementing primary measures could also be valuable for better understanding the potential outcomes of these measures.

Moreover, this could help determine the optimal placement, the number of injection points, the appropriate concentration of NH_3, and the extent of ammonia slip for both water-diluted ammonia injection and dissolver off gas. It may also facilitate the selection of the most effective SNCR method for reducing NO_x and other emissions.

Regarding the recycling of scrubber effluent, enhanced modelling and experimentation could improve the predictability of NO_x reduction and its impact on sulphidity in the flue gas, as well as dust formation. This approach would also reduce significant uncertainties arising from assumptions made based on the literature, such as the rate of dust recycling.

Bibliography

[1] Naturvårdsverket. "Nitrogen oxides, emissions to air". In: (2023). [Cited 2024-01-31]. URL: https://www.naturvardsverket.se/data-och-statistik/luft/utslapp/utslapp-av-kvaveoxider-till-luft/.

[2] European Environment Agency. *Air pollution in Europe: 2023 reporting status under the National Emission reduction Commitments Directive*. [Cited 2024-01-25]. Sept. 2023. URL: https://www.eea.europa.eu/publications/national-emission-reduction-commitments-directive-2023/air-pollution-in-europe-202.

[3] Naturvårdsverket. "Förslag till förändrad NOx-avgift". In: (2022). [Cited 2024-03-21]. URL: https://www.naturvardsverket.se/4acb9a/contentassets/7caf92437f0f4e828cd2ee35f91254b1/forslag-till-forandrad-nox-avgift.pdf.

[4] Suhr M, Klein G, Kourti I, Gonzalo MR, Santonja GG, Roudier S, and Sancho LD. *Best Available Techniques (BAT) Reference Document for the Production of Pulp, Paper and Board*. [Cited 2024-01-21]. 2015. DOI: doi:10.2791/370629.

[5] Hasani M. *Lignocellulose – Kraft process [PowerPoint presentation on the Internet]*. Gothenburg: Chalmers; 2023. [Cited 2024-01-17]. 2023. URL: https://chalmers.instructure.com/courses/20234/files/2291898?module_item_id=302574.

[6] Gonzaléz VM, Bayón RM, Antón JC, García-Gonzalo E, and Nieto PJ. "Predictive model of gas consumption and air emissions of a lime kiln in a kraft process using the ABC/MARS-based technique". In: *The International Journal of Advanced Manufacturing Technology* 100.5-8 (2019). [Cited 2024-01-17], pp. 1549–1562. ISSN: 0268-3768. DOI: 10.1007/s00170-018-2773-4.

[7] Tran H and Vakkilainen E. "The Kraft Chemical Recovery Process". In: (Feb. 2016). [Cited 2024-01-20].

[8] Patt R, Kordsachia O, Süttinger R, Ohtani Y, Hoesch JF, Ehrler P, and et al. "Paper and Pulp". In: (2000). [Cited 2024-01-17]. DOI: 10.1002/14356007.a18_545.

[9] Damasceno A, Carneiro L, Andrade N, Vasconcelos S, Brito R, and Brito K. "Simultaneous prediction of steam production and reduction efficiency in recovery boilers of pulping process". In: *Journal of Cleaner Production* 275 (2020). [Cited 2024-04-05], p. 124103. ISSN: 0959-6526. DOI: https://doi.org/10.1016/j.jclepro.2020.124103. URL: https://www.sciencedirect.com/science/article/pii/S0959652620341482.

[10] Hupa M. "Recovery boiler chemical principles". In: *TAPPI Kraft Recovery Course 2007* 2 (Jan. 2007). [Cited 2024-01-21]. URL: https://www.tappi.org/content/events/08kros/manuscripts/4-4.pdf.

[11] Quinde A. "The role of sulfidity during kraft pulping". In: (2021). [Cited 2024-04-04]. URL: https://www.pulpandpapercanada.com/the-role-of-sulfidity-during-kraft-pulping/.

[12] Lecomte T, Ferrería JF, Neuwahl F, Canova M, Pinasseau A, Brinkmann T, Jankov I, Roudier S, and Sancho LD. *Best Available Techniques (BAT) Reference Document for Large Combustion Plants*. [Cited 2024-02-10]. 2017. DOI: doi:10.2760/949.

[13] Esa K Vakkilainen. *Kraft recovery boilers - Principles and practice*. [Cited 2024-01-21]. Suomen Soodakattilayhdistys r.y., 2005. ISBN: ISBN 952-91-8603-7.

[14] Gall D, Allgurén T, Johansson J, Normann F, Heijnesson AH, Gunnarsson A, and Andersson K. "Recirculation of NOx and SOx Scrubber Effluent to an Industrial Grate Fired MSW Boiler-Influence on Combustion Performance, Deposition Behavior, and Flue Gas Composition". In: *Energy & Fuels* 36 (11 June 2022). [Cited 2024-03-06], pp. 5868–5877. ISSN: 0887-0624. DOI: 10.1021/acs.energyfuels.2c00293.

[15] Hakkarainen T. "Reduction of nitrogen oxide emissions in the lime kiln [MSc]". In: (2014). [Cited 2024-01-18]. URL: https://lutpub.lut.fi/handle/10024/102230.

[16] Adams TN, Frederick WJ, Grace TM, Hupa M, Iisa K, and Jones AK et al. *Kraft Recovery Boilers*. [Cited 2024-01-26]. TAPPI Press; 1997.

[17] Forssén M, Kilpinen P, and Hupa M. "NOx reduction in black liquor combustion - reaction mechanisms reveal novel operational strategy options". In: (1998). [Cited 2024-01-23]. URL: https://www.tappi.org/content/events/08kros/manuscripts/5-1a.pdf.

[18] Vähä-Savo N. "Behavior of Black Liquor Nitrogen in Combustion - Formation of Cyanate". [Cited 2024-01-18]. PhD thesis. Finland, 2014. ISBN: 978-952-12-3135-3.

[19] Lundberg M, Niemi P, Maîtrejean L, Yrjas P, Laurén T, Brink A, and Mikko Hupa. "Effect of ammonia injection on black liquor recovery boiler NOx emissions and ash chemistry". In: *TAPPI Press - Engineering, Pulping and Environmental Conference 2008*. TAPPI Press - Engineering, Pulping and Environmental Conference 2008. [Cited 2024-04-04]. 2008, pp. 1437–1458. ISBN: 9781605605081.

[20] Södra Cell Mönsterås Internal reports.

[21] Johansson J, Normann F, Sarajlic N, and Andersson K. "Technical-Scale Evaluation of Scrubber-Based, Co-Removal of NOx and SOx Species from Flue Gases via Gas-Phase Oxidation". In: *Industrial & Engineering Chemistry Research* 58 (48 Dec. 2019). [Cited 2024-02-05], pp. 21904–21912. ISSN: 0888-5885. DOI: 10.1021/acs.iecr.9b04791.

[22] Södra Cell Mönsterås Distributed Control System.

[23] Inc AspenTech. "Aspen physical property system". In: (2007). [Cited 2024-03-29].

[24] Ahlroth M, Andersson L, and Puukko M. "Studie av imångornas innehåll och inverkan på NOX-emissionen från sodapannor". In: (2011). [Cited 2024-05-14].

A

Appendix 1

Mass and energy balances

This appendix presents the tables and calculations used for validating the mass and energy balances in the base case. The method used for the calculations is based on Chapter 1 in the book Kraft Recovery Boilers [16]. Table A.1 shows the same elemental composition of the black liquor entering the recovery boiler as in Table 3.1.

Table A.1: Sample composition of black liquor (concentrated product).

	A	B	C
1	Element		wt% BLS
2	Carbon	C	31.40 %
3	Hydrogen	H	3.710 %
4	Nitrogen	N	0.060 %
5	Chloride	Cl	0.160 %
6	Sulphur	S	4.590 %
7	Oxygen	O	37.74 %
8	Sodium	Na	20.34 %
9	Potassium	K	2.000 %

Table A.2 presents all the given and assumed operating conditions needed for the mass and energy calculations for Södra's recovery boiler. It includes the necessary data for black liquor, air, steam and water, flue gas, smelt, and dust.

Table A.2: Sample operating parameters for mass and energy balances.

	A	B	C	D
10		Item	Metric	Units
11	Black liquor	Reduction efficiency	94.00	%
12		Total flow	66.82	kg/s
13		Dry BL flow (BLS)	50.12	kg/s
14		DS	75.00	%
15		Temperature	141.0	℃

Continued on next page

	A	B	C	D
16		Cp	2.800	kJ/(kg·K)
17		LHV	12.45	MJ/kg
18		HHV	13.54	MJ/kg
19				
20	Air	Cp	1.006	kJ/(kg·K)
21		Air flow ($1^{st} + 2^{nd}$)	107.5	Nm^3/s
22		Air flow ($3^{rd} + 4^{th}$)	42.99	Nm^3/s
23		DNCG flow	11.90	Nm^3/s
24		Temperature ($1^{st} + 2^{nd}$)	165.0	℃
25		Temperature ($3^{rd} + 4^{th}$)	30.00	℃
26		Temperature (DNCG)	90.00	℃
27		O2 mass fraction	0.2320	
28		N2 mass fraction	0.7680	
29		O2 mole fraction	0.2100	
30		N2 mole fraction	0.7900	
31				
32	Steam/water	Steam production	174.0	kg/s
33		Feedwater temperature	124.0	℃
34		Cp water	4.190	kJ/(kg·K)
35		Reference temp. (air and water)	25.00	℃
36		Saturated water enthalpy (25°C)	104.8	kJ/kg
37		Water heat of vaporisation (25°C)	2443	kJ/kg
38		Steam temperature	480.0	℃
39		Steam pressure	61.00	bar
40		Enthalpy of steam (61 bar, 480 ℃)	3373	kJ/kg
41		Saturated steam enthalpy (61 bar)	2770	kJ/kg
42		Cp steam	1.900	kJ/(kg·K)
43		Enthalpy blowdown	1150	kJ/kg
44				
45	Flue gas	Cp (dry)	1.000	kJ/(kg·K)
46		Cp (wet)	1.410	kJ/(kg·K)
47		Outlet temperature	195.0	℃
48		Reference temperature	200.0	℃
49		CO (dry flue gas)	368.0	ppmv
50		SO2 (dry flue gas)	0.0025	ppmv
51		TRS (H2S, dry flue gas)	0.0026	kg/s
52		Pressure (P)	101.3	kPa
53		Gas constant (R)	8.314	J/(mol·K)
54		Temperature (T)	273.2	℃
55				
56	Smelt	Specific enthalpy (smelt)	1350	kJ/kg
57		Specific enthalpy (Na_2S)	12900	kJ/kg
58				

Continued on next page

	A	B	C	D
59	Dust	Particulate loading	0.0002	kg/Nm^{3}tg
60		Dust recycle	10.00	% of initial Na
61		Converter (Nm^3 → kg/s)	0.0422	kmol/kg
62		S in dust	18.98	%
63		Na in dust	31.81	%
64	CNCG	Sulphur in CNCG flow	0.0657	kg/s

Table A.3 shows the molar masses of the elements and compounds required for the calculations.

Table A.3: Molar masses needed for calculation.

	A	B	C
65	Element/Compound		g/mol
66	Sodium carbonate	Na_2CO_3	106.0
67	Sodium sulphate	Na_2SO_4	142.0
68	Potassium sulphate	K_2SO_4	174.3
69	Potassium carbonate	K_2CO_3	138.2
70	Sodium chloride	NaCl	58.44
71	Hydrochloric acid	HCl	36.46
72	Sodium sulphide	Na_2S	78.04
73	Sodium	Na	22.99
74	Carbon	C	12.01
75	Oxygen	O_2	15.99
76	Sulphur	S	32.06
77	Potassium	K	39.10
78	Hydrogen	H	1.008
79	Chlorine	Cl	35.45
80	Carbon dioxide	CO_2	44.01
81	Carbon monoxide	CO	28.01
82	Water	H_2O	18.02
83	Nitrogen gas	N_2	28.02
84	Suphur dioxide	SO_2	64.07
85	Total reduced sulphur	TRS (H_2S)	34.08
86	Hydrogen gas	H_2	2.016
87	Air	Air	28.84

Table A.4 outlines the calculations for the smelt composition, stoichiometric combustion products, and the oxygen required for the different compounds in the boiler. The numbers listed in many of the calculations tables are in kg based on 50.115kg of dry black liquid solids (BLS) input to the boiler.

Table A.4: Smelt and stoichiometric combustion products.

	A	B		C
89		Item	Calculation	kg/50 kg BLS
90	Smelt	Na_2S	$C13 \cdot C11 \cdot (C71/C75) \cdot C6$	5.263
91		Na_2SO_4	$C13 \cdot (1 - C11) \cdot C6 \cdot (C66/C75)$	0.6114
92		NaCl	$C13 \cdot C5 \cdot (C69/C78)$	0.1322
93		Na_2CO_3	$C13 \cdot (C65/(C72 \cdot 2)) \cdot (C8-(2 \cdot C72/C75) \cdot C6-(C72/C78) \cdot C5)$	15.77
94		K_2CO_3	$C13 \cdot C9 \cdot (C68/(2 \cdot C76))$	1.771
95		Total Smelt	$SUM(C90 : C94)$	23.55
96				
97	Stoichiometric combustion products	CO_2	$(C79/C73) \cdot (C13 \cdot C2-(C73/C65) \cdot C93-(C73/C68) \cdot C94)$	50.53
98		H_2O	$C13 \cdot C3 \cdot (C81/2)$	16.73
99				
100	Oxygen requirement	O_2 for Na_2SO_4	$C91 \cdot (C74 \cdot 4/C66)$	0.2755
101		O_2 for Na_2CO_3	$C93 \cdot (C74 \cdot 3/C65)$	7.143
102		O_2 for K_2CO_3	$C94 \cdot (C74 \cdot 3/C68)$	0.6152
103		O_2 for CO_2	$C97 \cdot (C74 \cdot 2/C79)$	36.75
104		O_2 for H_2O	$C98 \cdot (C74/C81)$	14.87
105		Total O_2	$SUM(C100 : C104)$	59.66

Table A.5 illustrates the total air requirement as well as the resulting flue gas flow. The water vapor in stack gas is simplified since it only considers water from the black liquor since it is the biggest source of water. The direct heating steam for liquor, the humidity in the air, and the sootblowing steam were neglected due to the difficulty in modelling this.

Table A.5: Air requirement and flue gas flow.

	A	B		C
106		Item	Calculation	kg/50 kg BLS
107	Air	O_2 in BLS	$C13 \cdot C7$	18.91
108		Total O_2 req.	C105	59.66
109		O_2 req. from air	$C108 - C107$	40.74
110		Stochiometric combustion air	$C109/C27$	175.6
111		N_2 in stochiometric combustion air	$C110 \cdot C28$	134.9
112		Total excess air (20% of stochiometric)	$C110 \cdot 0.2$	35.12
113		Total air flow	$C110 + C112$	210.7
114		Tot air flow	$(C113/((C83 \cdot C29 + C82 \cdot C30) \cdot C53 \cdot C54))/C52$	163.8 Nm^3/s
115		Primary air req. for RE	$((((C100 + C101 + C102)/C83) \cdot C53 \cdot C54)/C52/C29)$	26.79 Nm^3/s
116				
117	Water vapor in stack gas	Steam in stack from water BL	$C13 \cdot (1 - C14)/C14$	16.71
118		Total added water vapor	C117	16.71
119				
120	Flue gas	Total Flue Gas Flow	$C97 + C98 + C111 + C112 + C118$	254.0

Table A.6 presents the composition of the flue gas both in wet-basis and dry-basis. The excess air used for combustion is measured in O_2% for the flue gas. This can also be reported in dry-basis or wet-basis and the difference is the approaches used when measuring, the more common measurement for recovery boilers today is wet-basis.

Table A.6: Flue gas composition.

	B		C	D
121	Item	Calculation		Units
122	Mol wt. of wet flue gas	$C120/(C97/C79+$ $C111/C82+C112/C87+$ $(C98+C118)/C81)$	28.09	
123	Total dry flow gas	$C97+C111+C112$	220.5	kg/50 kg BLS
124	Mol wt. of dry flue gas	$C123/(C97/C79+$ $C111/C82+C112/C87)$	30.69	
125	Total excess oxygen	$C112 \cdot C27$	8.149	kg/50 kg BLS
126	O_2 % in wet flue gas	$C125/C83/(C120/C122)$	2.816	%
127	H_2O % in wet flue gas	$(C98+C118)/C81/$ $(C120/C122)$	20.54	%
128	CO_2 % in wet flue gas	$C97/C79/(C120/C122)$	12.70	%
129	N_2 % in wet flue gas	$1-C126-C127-C128$	63.94	%
130	O_2 % in dry flue gas	$C125/C83/(C123/C124)$	3.544	%
131	CO_2 % in dry flue gas	$C97/C79/(C123/C124)$	15.98	%
132	N_2 % in dry flue gas	$1-C130-C131$	80.47	%

Table A.7 shows the carbon and hydrogen conversion efficiencies. The purpose of combustion is to convert all hydrogen to H_2O and all carbon to CO_2 or carbonate. CO, H_2 in the flue gas, and carbon in the smelt are considered inefficiencies. Hydrogen's conversion to H_2O is assumed to be 100%, but the actual value was 99.9%. The table also contains total sulphur and sodium in the boiler as well as the losses. The amount of sulphur in stack TRS is taken from Södra's environmental report (2023).

Table A.7: Conversion efficiencies and losses.

	A	B		C
133		Item	Calculation	kg/50 kg BLS
134	C and H efficiencies	Conversion to H_2O	-	100.0 %
135		CO in the flue gas	$C49 \cdot 10^{-6} \cdot C80 \cdot C123/C124$	0.0740
136		C in smelt (1 wt% of smelt)	$0.01 \cdot C95$	0.2355
137		Total C available for combustion	$C97 \cdot (C73/C79)$	13.79
138		% C converted to CO_2	$(1 - C136/C137 - (C73/C80) \cdot C135/C137)$	98.06 %
139		% C in the smelt	$C136/C137$	1.710 %
140		% C to CO	$(C73/C80) \cdot C135/C137$	0.2302 %
141				
142	S Loss from RB	Total S to RB	$(C13 \cdot C6) + C64$	2.366
143		S in stack SO_2	$C50 \cdot 10^{-6} \cdot C123 \cdot (C75/C124)$	$0.5640 \cdot 10^{-6}$
144		S in stack TRS	C51	$0.2417 \cdot 10^{-4}$
145		Stack particulate flow	$C59 \cdot C123/(C61 \cdot C124)$	0.0341
146		S in stack particles	$C62 \cdot C145$	0.0065
147		% S loss	$(C143 + C144 + C146)/C142$	0.3808 %
148		S in dust cycle	$C13 \cdot C8 \cdot C60 \cdot C62/C63$	0.6082
149		Total S in flue gas	$C148 + C143 + C144$	0.6107
150		% S in flue gas not oxidised	$C144/C149$	0.0040 %
151				
152	Na loss from RB	Total Na to boiler	$C13 \cdot C8$	10.19
153		Na in stack particulate	$C145 \cdot C63$	1.083 %
154		% Na loss	$C153/C152$	0.1063 %
155		Total Na in flue gas	$C13 \cdot C8 \cdot C60$	1.019

Table A.8 presents the energy balance in the boiler with all the heat input and heat output. The numbers are reported in both kJ/kg BLS and MW. Once again, neither the heat input nor heat output is considered in feedwater for sootblowing steam nor in feedwater for blowdown in the energy balance.

Table A.8: Energy balances for a black liquor recovery boiler.

	A	B		C	D
156		Item	Calculation	kJ/kg BLS	MW
157	Heat input	Heating value of BLS	$C17 \cdot 1000$	12450	623.9
158		Sensible heat in BL	$(1/C14) \cdot C16 \cdot (C15 - C35)$	433.07	21.70
159		Sensible heat in air $(3^{rd} + 4^{th})$	$((C22/C114) \cdot C113/C13) \cdot C20 \cdot (C25 - 25)$	5.5522	0.2783
160		Heat to preheat air $(1^{st} + 2^{nd})$	$((C21/C114) \cdot C113/C13) \cdot C20 \cdot (C24 - C35)$	388.82	19.49
161		Heat to preheat DNCG	$((C23/C114) \cdot C113/C13) \cdot C20 \cdot (C26 - C35)$	19.980	1.001
162		Total heat input	$C157 + C158 + C159 + C160 + C161$	13297	666.4
163					
164	Heat Output	Sensible heat in dry flue gas	$(C123/C13) \cdot C45 \cdot (C47 - C24 + C35)$	242.04	12.13
165		Heat loss from H_2 in BLS	$(C98/C13) \cdot (C41 + C42 \cdot (C47 - C48))$	921.73	46.19
166		Sensible heat in smelt	$(C95/C13) \cdot C56$	634.42	31.79
167		Heat to form sulphide	$(C90/C13) \cdot C57$	1354.8	67.90
168		Radiation loss (0.3% of heat input)	$C162 \cdot 0.003$	39.892	1.999
169		Unaccounted losses (1.5% of heat input)	$C162 \cdot 0.015$	199.46	9.996
170		Total losses	SUM$(C164 : C169)$	3392.3	170.0
171		Heat to steam	$C162 - C170$	9905.1	496.4
172		Total heat output	$C170 + C171$	13279	666.4

B

Appendix 2

Primary measure

B.1 Dissolver off gas

Table B.1 presents the given operating conditions for the dissolver off gas from Södra. $NO_{initial}$ is based on the total NO_x emissions and the total flue gas flow from DGE's report.

Table B.1: Operating parameters for dissolver off gas.

	B	C	D
1	Item	Metric	Units
2	Temperature	341.0	°C
3	Density	0.9940	kg/m^3
4	Enthalpy	524.6	kJ/kg
5	Total mass flow	13.34	kg/s
6	H_2O in air	2.034	kg/s
7	Air flow	11.30	kg/s
8	Molar mass NH_3	17.03	g/mol
9	NOx initial	0.7547	mol/s
10	Dry flue gas flow	197.3	Nm^3/s

Table B.2 shows the calculations for the water and air content in the dissolver off gas and the conversion of fuel nitrogen to NH_3 concentration.

Table B.2: Calculations for dissolver off gas and NH_3.

	B		C	D
12	Item	Calculation	Metric	Units
13	Water content	$B6/B5$	0.1524	wt%
14	Air content	$B7/D5$	0.8420	wt%
15	N in fuel	-	108.0	kg/h
16	N in char (OCN^-)	$B15/3$	36.00	kg/h
17	NH_3 (50% OCN^-)	$B16/2$	18.00	kg/h
18		$B17/0.0036$	5000	mg/s
19		$(B17/3.6)/B8$	0.2936	mol/s
20	mol NH_3/mol NO_x	$B19/B9$	0.3890	
21	NH_3 concentration in dry flue gas	$B18/B10$	25.34	mg/Nm^3

B.2 Scrubber effluent

Table B.3 presents the actual elements and compounds in the effluent stream leaving the scrubber, and their flows in kmol/h. HADS contains 1 nitrogen, 2 sulphur and 7 oxygen.

Table B.3: Original scrubber effluent.

	I	J
1	Effluent	kmol/h
2	NO_2	$3.81 \cdot 10^{-10}$
3	SO_2	$7.27 \cdot 10^{-13}$
4	N_2	$1.05 \cdot 10^{-3}$
5	H_2O	$2.44 \cdot 10^{2}$
6	HNO_2	$2.99 \cdot 10^{-2}$
7	HNO_3	$8.62 \cdot 10^{-4}$
8	HSO_3^-	$3.80 \cdot 10^{-6}$
9	SO_3^{2-}	$1.03 \cdot 10^{-3}$
10	NO_2^-	$9.09 \cdot 10^{-1}$
11	NO_3^-	$1.39 \cdot 10^{-3}$
12	H^+	$3.49 \cdot 10^{-8}$
13	H_2SO_4	$4.42 \cdot 10^{-24}$
14	HSO_4^-	$1.27 \cdot 10^{-7}$
15	Na^+	8.40
16	OH^-	$2.95 \cdot 10^{-4}$
17	CO_2	$5.04 \cdot 10^{-3}$
18	HCO_3^-	1.51
19	SO_4^{2-}	1.21
20	CO_3^{2-}	$2.81 \cdot 10^{-1}$
21	O_2	$9.21 \cdot 10^{-5}$
22	HADS	1.49

Table B.4 presents the conversion of the ionic elements and compounds to a scrubber effluent containing only N_2, Na_2SO_4, CO_2, and H_2O.

Table B.4: Converted scrubber effluent.

	I		J
23	Converted effluent	Calculation	kmol/hr
24	N_2	$((J2+J6+J7+J10+J11+J22)/2) + J4$	1.220
25	Na_2SO_4	$(J3+J8+J9+J14+J19)+(J22 \cdot 2)$	4.200
26	CO_2	$J17 + J18 + J20$	1.796
27	H_2O	$J5$	243.9

DEPARTMENT OF SPACE, EARTH AND ENVIRONMENT
CHALMERS UNIVERSITY OF TECHNOLOGY
Gothenburg, Sweden
www.chalmers.se

CHALMERS
UNIVERSITY OF TECHNOLOGY